Master's Thesis

Predicting Types of Driver

by

Tung Huynh

A thesis submitted to the Department of Computer Science,
College of Natural Sciences and Mathematics
in partial fulfillment of the requirement for the degree of
Master of Science
in Computer Science

Chair of Committee: Ioannis Pavlidis
Committee Member: Guoning Chen
Committee Member: Michael Manser

University of Houston
August, 2020

Acknowledgements

I wish to express my sincere appreciation to my advisor, Professor Ioannis Pavlidis, who guided and encouraged me to keep exploring and moving forward even when the road got tough. His sharing of knowledge and guidance helped me do the right analysis and connect the things. Without his persistent help, the goal of this project would not have been achieved.

I also wish to express my gratitude to my committee members, Dr. Guoning Chen and Dr. Michale Manser, who gave me their comprehensive review and suggestions on this thesis.

I also wish to acknowledge the support of all members of the Computational Physiology Lab. I am grateful that they not only shared their understanding of the precious data and technical support on data processing steps but also contributed their suggestions on the predicting models of this thesis.

Abstract

Driver types and their associated behaviors not only shape our driving habits but our reactions in unintended driving events as well. The open road places us in unexpected situations and forces us to act and react in particular ways. Here, in this thesis, I propose a method to predict the types of drivers and their associated reactions during unintended events. We demonstrate our clustering and predicting methods with data from two simulations, On-road Driving (ORD) and Test Track Driving 1 (TTD1). In the On-road Driving study ($n = 8$), we construct a between-variable predicting model to predict the level of arousal of perinasal perspiration for the next 5 seconds based on driving variables of the last 30 seconds. Subsequently, we use TTD1 ($n = 21$) data to develop a within-variable model to predict the arousal of drivers during an unintended acceleration event based on their arousal levels in driving tests simulating our daily driving. We achieve a classification performance AUC at 0.96 and 0.90 for between-variable prediction model and within-variable predicting model, respectively. We also find a group of accelerophobic drivers whose stress level increases along with the acceleration of vehicles. The proposed method can also be used in the design of future vehicles; the types of drivers could be detected and embedded in advanced automation systems to personalize car driving variables or enhance car safety features accordingly.

Table of Contents

List of Tables

List of Figures

Chapter 1

Introduction

1.1 Literature Context

In 2019, car accidents claimed 38,800 lives and caused 4.4 million injuries. Both human factors and machine factors contributed to these accidents. However, driver-related behavioral factors were present in 95% of all accidents (Petridou and Moustaki, 2000). Shinar introduced the role of psychology in highway safety in a systematic manner, pointing out that people drive the way they live (Shinar, 1978). Among the many types of drivers, anxious drivers and stress-prone drivers may place themselves and others at an increased risk of accidents (Clapp et al., 2011). Researchers have shown that anxiety is a positive predictor of drivers' flaws in drivers of all ages (Lucidi et al., 2019). Notably, in case of sudden unintended acceleration (SUA) (Park, Choi, and Choi, 2016), which causes 16.000 accidents yearly (NHTSA, 2015), this type of driver might find it more difficult to handle the situation.

In recent years, driver types, characteristics, and associated behaviors have been the subject of research attention. While one group of researchers has focused on the short-term state of drivers (such as aggressiveness, distraction, drowsiness, or stress levels), the other group has studied drivers' long-term characteristics (Eboli, Mazzulla, and Pungillo, 2017). In the former group, researchers has used physiological monitoring systems and visual tracking systems to detect a driver's state. For example, a driver's physiological signals could indicate distraction, aggressiveness (Panagopoulos

and Pavlidis, 2020), and stress levels (Healey and Picard, 2005; Saeed and Trajanovski, 2017). Mirror glance patterns and eye movement also predict lane changing and driving around curves (Beggiato et al., 2017; Ren et al., 2015). In the latter group, researchers mainly extract the drivers' characteristics from demographic information and past traffic violations, as these factors can help to predict vehicle crashes (Kim, Ramjan, and Mak, 2015).

1.2 Our Work

Our primary research goal in the present study was to discriminate between types of drivers based on analyzing the changes in human physiology in relation to vehicle variables. Moreover, from this analysis, we built a short-term prediction model of driver stress based on driving variables and a long-term prediction model of a reaction during a catastrophic event based on typical daily driving behaviors. To complete this research goal, we used data from the On-road Driving (ORD) study and the Test Track Driving 1 (TTD1) study. While the advantage of the ORD study is that it simulates daily driving on highways and residential streets, the TTD1 study is a controlled study consisting of multiple driving tests under different types of stressors, including cognitive stressors, sensorimotor stressors, and a simulated catastrophic event.

With the ORD study, we built a between-variable prediction model that used driving variables such as speed, acceleration, brake force, and steering angle to predict drivers' arousal via perinasal perspiration. For this purpose, we segmented the time-series data of each driver's arousal via perinasal perspiration and driving variables into five-second windows. After we applied feature engineering techniques to arrive at a representative set of all signals, we fed these features into a clustering model and a prediction model. While the clustering algorithm discriminated between groups of drivers on whom driving variables had a similar impact on, the predicting model was

able to precisely predict the trends of arousal in the next five seconds based on the driving variables of the last five seconds. Our approach in this study revealed a group of $accelerophobic$ drivers who showed a fear of acceleration but not of speed.

With the TTD1 study, we only leveraged the arousal and type of stressors to build a within-variable prediction model. We used the definition of $accelerophobic$ drivers that we found in the ORD study to segment the arousal based on acceleration levels. Accordingly, we also preprocessed and performed feature engineering on arousal in driving tests with applicable stressors, including normal, cognitive, and motoric. Subsequently, we fed these features into a classification model with the XGBoost algorithm to predict the level of arousal change during and after an unintended acceleration event (or "catastrophic event"). Interestingly, not only did the prediction model show precise predictions, but our analysis also revealed a close association between groups of drivers in driving tests with groups of drivers at the catastrophic event.

We organize the remainder of the thesis as follows:

- In chapter 2, we present our approach for discriminating between types of drivers and a short-time prediction model of drivers' stress levels on data of the On-road Driving study. This chapter consists of four sections: study design, database, methods, and results.

- In chapter 3, based on the types of drivers associated with acceleration that we found from data of the On-road Driving study, we describe about a prediction model to forecast the drivers' stress levels in a catastrophic event in the Test Track Driving 1 (TTD1) study. This chapter also consists of four sections: study design, database, methods, and results.

- In chapter 4, we discuss the common findings obtained from the two studies and conclude this work. We also discuss about the applications of our results and future research direction.

Chapter 2

On-road Driving Study

2.1 Study Design

2.1.1 Subjects

At the beginning of this study, we used emails and flyer postings to recruit subjects from the communities of Bryan and College Station, Texas. These subjects had to have a healthy vision and a valid driving license. We only selected individuals with at least one and a half years of driving experience. Those subjects were from 18 to 27 years old. To enhance driving safety, we excluded subjects who were taking medications affecting their driving ability. A total of $n = 12$ subjects conforming to the inclusion-exclusion criteria volunteered for the study. Raw data for $n = 4$ subjects were not adequately recorded due to technical issues or due to significant problems with extracting perinasal perspiration signals. Hence, our final working set consists of nearly-complete raw data for $n = 8$ subjects (three males/ five females).

2.1.2 Experimental Setup

The On-road Driving study consists of a baseline session and an on-road driving session. During these experimental sessions, the systems continuously imaged the participants' faces with a thermal and visual camera. The systems also captured participants'

physiological signals with a wearable device. Simultaneously, a driving data acquisition system recorded vehicle driving variables. A detailed description of each system is given below:

2.1.2.1 Sensors for Human

- *Thermal facial camera.* We used a Tau 640 long-wave infrared (LWIR) camera (FLIR Commercial Systems, Goleta, CA); it features a small size $(44 \times 44 \times 30\ \mathrm{mm})$ and adequate thermal $(< 50\ \mathrm{mK})$ and spatial resolution $(640 \times 512$ pixels$)$. The 640 camera was outfitted with an LWIR $35\ \mathrm{mm}$ lens $f/1.2$. Thermal data was collected at a frame rate of 7.5 fps. We used these thermal facial videos to extract perinasal perspiration signals, known to commensurate with electrodermal (EDA) activity in the palm. For this reason, we call the thermally extracted perinasal perspiration signals, *perinasal EDA signals*.

- *Visual facial camera.* A Logitech HD Pro - C920 camera (Logitech, Newark, CA) with spatial resolution 1920×1080 pixels and a frame rate of 30 fps. It is placed $1\ \mathrm{m}$ from drivers, tucked atop driver's side car dashboard (Figure 2.1). The distance in combination with the camera optics ensured that a typical face covered a significant portion of each thermal and visual frame, providing maximum spatial resolution for image analysis.

- *Visual dash camera.* This camera was placed on the car dash, aiming at the front view of the car, to record the subject's drive. We use a Logitech Brio camera (Logitech, Newark, CA) with spatial resolution 1280×720 pixels and a frame rate of 30 fps.

We also collected additional physiological data via a sensor specified as follow:

- *Adrenergic sensor.* We used the Zephyr BioHarness 3.0 (Zephyr Technology, Annapolis, MD) sensor to measure the subject's heart rate and breathing rate-two standard indicators of adrenergic control. The sensor connects to a chest strap that is worn underneath the subject's clothing. It is powered by a rechargeable

lithium polymer battery (up to 26 h per charge) and is capable of detecting a heart rate range of $25 - 240$ bpm and a breathing rate range of $4 - 70$ bpm.

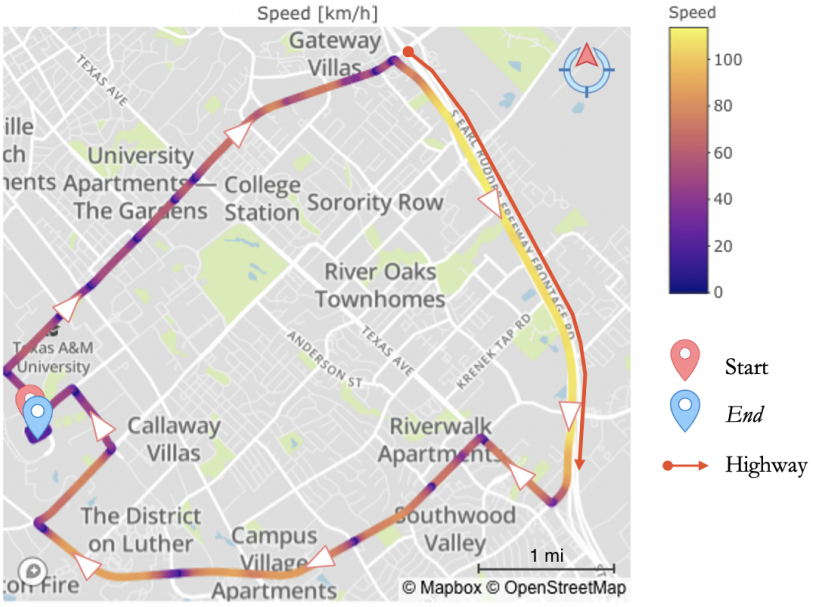

(A)

(B)

FIGURE 2.1: Study design of On-road Driving study
(A) Full itinerary of on-road driving (ORD) experiment around the College Station, TX. The white arrows indicate the direction of driving. This map is generated with Plotly and Mapbox library using data from OpenStreetMap (OpenStreetMap Contributors, 2017) (B) Physiological sensors and camera setup in a car.

2.1.2.2 Sensors for Vehicle

Importantly, we used a Dewetron Data Acquisition (DAQ) system to record driving variables from different channels. These variables included speed, acceleration, brake force, and steering angle. This Dewetron unit included a high-precision quartz-stabilized system running at a frequency of 80 MHz and generating a slope accuracy of 2 ns. Additionally, it also collected absolute time geographic location information from a GPS acquisition module.

2.1.3 Experimental Design

Upon signing the consent form, the subjects completed questionnaires to identify demographic information including gender and age. The subjects then participated in two experimental sessions. The design of the two sessions was as follows:

- *Baseline session (BL).* Subjects only sat quietly in a parked car and listened to soothing music for about five minutes. As the car was not moving, only the physiological sensors ran and captured the physiological signals from subjects during this session.

- *On-road drive session (ORD).* Subjects participated in a drive around College Station, Texas. Figure 2.1(A) shows the full itinerary of this driving session. This itinerary consisted of a segment of Texas State Highway 6 as well as residential streets. It took 25-35 minutes for subjects to complete this 12-mile journey. The subject's car traveled in the right-hand lane at a speed in the range of [0-120] kph, equivalent to [0-75] mph.

2.1.4 Signal Extraction

2.1.4.1 Tissue Tracking and Perinasal Perspiration Signal Extraction

We used a tissue tracker reported by Zhou et al. (Zhou et al., 2013). Initially, we initiated the tracking algorithm by selecting the subject's perinasal region in the first frame. In every subsequent frame, the tracker determined the best matching section of the

thermal clip via spatiotemporal smoothing. In the selected and matching region of the thermal images, activated perspiration pores appeared as "cold" (dark) spots, amidst "hot" surrounding tissue (Figure 2.2). Finally, to compute the perspiration signal, we applied a morphology-based algorithm to the measurement region of interest (MROI) (Shastri et al., 2012).

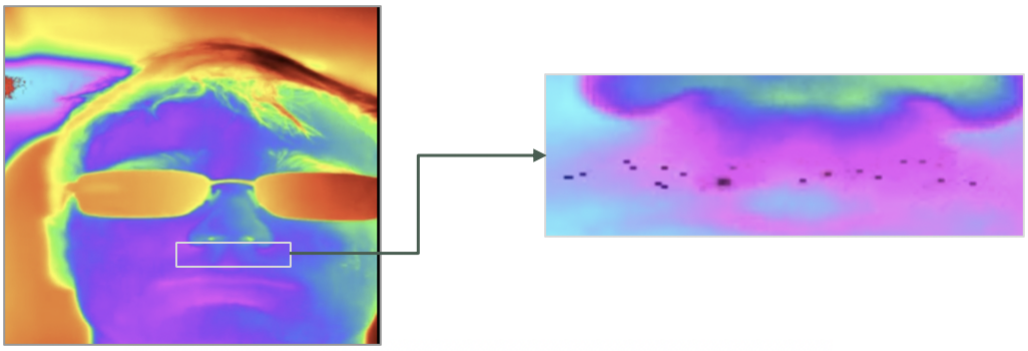

FIGURE 2.2: Perinasal Perspiration Signal Extraction

2.1.4.2 Driving Data Extraction

All incoming driving signals were filed in a single database. These included speed, acceleration, brake force, steering angle, pulse-per-second (PPS) signal of a GPS satellite, and time-related information. We used Dewesoft, a data acquisition software, to extract tabular data from the database.

2.2 Database

We publicly hosted quantitative data and videos of On-road Driving Study on a Open Science repository at *https://osf.io/974vf/*.

2.2.1 Quantitative Data

The quantitative data folder holds comma separated value (csv) file. In the data summary file, in addition to the columns showing the row number (Column A) and Time

(Column B), there are columns holding physiological data (Columns C - H), columns holding vehicle variables (Columns I - M), and columns holding geographic variables (Columns N - O).

- $Column\ C$: PP - Values of the perinasal perspiration signal in $^{\circ}C^{2}$.
- $Column\ D$: PP_NR - Value of perinasal perspiration after using Low-pass Filtering method to suppress noise.
- $Column\ E$: HR - Values of the heart rate signal in BPM, measured with the BioHarness in subjects' chest.
- $Column\ F$: BR - Values of the breathing rate signal in BPM, measured with the BioHarness in the subjects' chest.
- $Column\ G$: SkinTemp - Skin temperature.
- $Column\ H$: Posture - Posture.
- $Column\ I$: PeakAccel - Peak acceleration force in %.
- $Column\ J$: Accelerator - Accelerator pedal force in %.
- $Column\ K$: Brake - Brake pedal force in %.
- $Column\ L$: Steering - Steering angle in $^{\circ}$.
- $Column\ M$: Speed - Speed in km/h.
- $Column\ N$: IN_Lat - Latitude.
- $Column\ O$: IN_Long - Longitude.

2.2.2 Video Data

Each folder in this folder consists of four video files for each subject. For baseline videos, subject only sat in the parking car in approximate five minutes without any tasks or types of stressor. For On-road Drive videos, subject drove on road around College Station, TX.

- $Subject00\_Baseline.avi1.avi$: Facial view of Baseline session.
- $Subject00\_Baseline.avi2.avi$: Front view of Baseline session.
- $Subject00\_OnRoadDrive.avi1.avi$: Facial view of On-road Driving session.
- $Subject00\_OnRoadDrive.avi2.avi$: Front view of On-Road Driving session.

2.3 Methods

2.3.1 Methodological Flow

In this study, we used all driving variables to form the study's exploratory variables. We aimed to analyze the impact of these factors on human physiology and characterize types of drivers based on the extent of the effects. We used instantaneous perspiration at the perinasal area as a proxy of the subject's sympathetic state (Pavlidis et al., 2016), thus forming the study's explained variable.

Figure 2.3 depicts the methodological flow of our approach. After preprocessing variables and extracting features, we built a linear model to show the overall effects of driving factors on drivers' arousal. Subsequently, we implemented a clustering algorithm to discriminate between different types of drivers in the study and built a machine learning (ML) model to predict each driver's arousal with time-series data. The remainder of this section describes the individual elements of the flow in more detail.

2.3.2 Preprocessing

Technical issues of sensors and human errors cause substantial problems with signal recording, especially physiological signals. Therefore, we had to apply some preprocessing techniques to clean and remove noises from these signals. Besides, the nature of signals also required us to standardize the dataset.

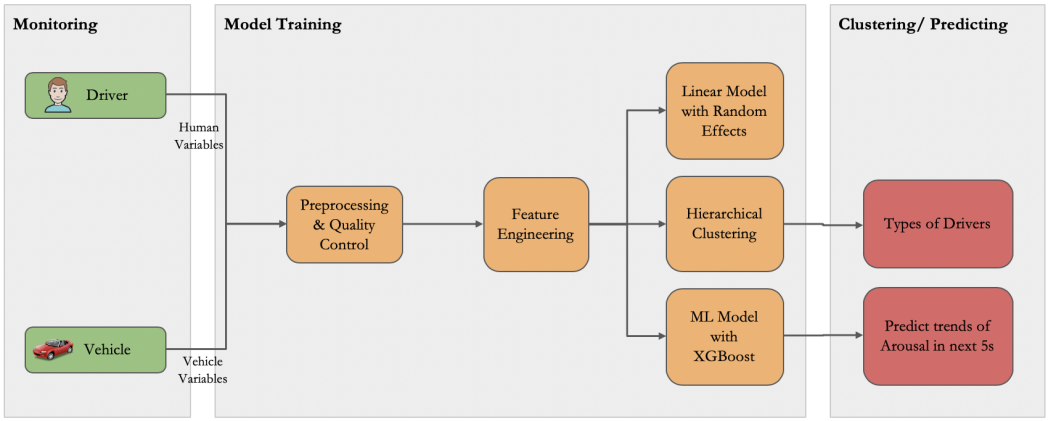

FIGURE 2.3: Overview of methodological flow
While the clustering of driver types was based on hierarchical clustering, the between-variable prediction model of drivers' arousal in the next five seconds used the driving variables in the past five seconds.

2.3.2.1 Quality Control

We applied the quality control method proposed in the paper of Zaman et al., 2019. Since we did not have any redundant channel modality, we only performed quality control level 1 (QC1), which indicates the application of a specification filter. In the case of signals from physiological probes, their values were checked to ascertain that they were within the specification range given by the sensor manufacturer. Signals that were found to have values outside of this range were discarded from the set.

2.3.2.2 Signal Smoothing with Fast Fourier Transform

Perinasal perspiration composes many different component signals at different frequencies. The perspiration signal also contains noise (Zhou et al., 2013). Therefore we used the low-pass filtering method, which is based on the fast Fourier transform (Sorensen et al., 1987) (FFT) for suppressing high-frequency signals. The FFT decomposes the original signal into many components with different frequencies by transforming it from time space to frequency space. Subsequently, we used a low-pass filter ($f = 1/2.5$) to eliminate high-frequency signals. Finally, we applied the inverse version of FFT to reconstruct the cleaned signal from extracted components. Figure 2.4 shows the perinasal perspiration before and after applying the filtering.

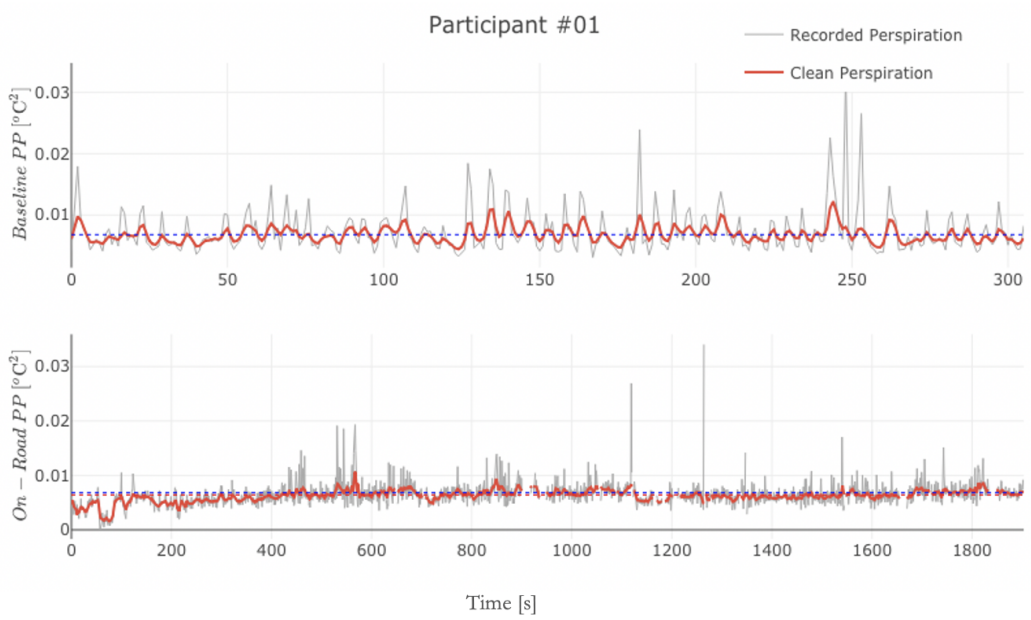

FIGURE 2.4: Original recorded and clean perinasal perspiration of $Subject$ #01 in BL and ORD sessions.
The blue hyphenated lines indicate the corresponding signal means.

2.3.2.3 Normalization

As the tonic level of arousal is known to vary significantly between individuals (Zhou et al., 2013), we computed each subject's arousal by subtracting perinasal perspiration with the mean of their baseline perspiration level. Equation 2.1 shows the formula of the normalization of arousal of subject i at time t of the ORD experimental session.

$$\Delta PP_{ORD_{it}} = ln(PP_{ORD_{it}}) - ln(\mu_{PP_{BL_i}}) \tag{2.1}$$

2.3.2.4 Resampling

Finally, we resampled all signals at 1 Hz. Although the perinasal perspiration signal extractor and Dewetron DAQ System can generate data at eight and 200 samples per second, respectively, to possibly incorporate with other physiological sensors, such as chest sensors measuring heart rate and breath rate, the frequency limits of which are 1 Hz.

2.3.3 Feature Extraction

We performed feature extraction in a time window of 10 seconds. This included extracting the driving variables in the past five seconds and computing the mean of arousal of each subject in the next five seconds. As response time varies for different types of physiological signals and the sensitivity capacity of DAQ, we chose an upper limit as the time window for feature extraction when incorporating all of these signals. In our experimental setup, systems recording human and driving variables ran at different frequencies. The Dewetron DAQ in which a high-precision quartz-stabilized system cycle with 80 MHz and a slope accuracy of 2 ns is generated (Huber and Drews, 2009). Perinasal perspiration is a cholinergic signal that is highly sensitive and manifests the onset of stress within two to five seconds (Tsiamyrtzis et al., 2016). Since we only used this physiological signal in our approach, we chose five seconds as the upper limit for the time window. We performed two types of feature from all driving variables and arousal as follows:

$$\Delta \mathrm{PP}_{\mathrm{ORD}_{i,t+5}} = f(Speed_{i,t}, Accel._{i,t}, Brake_{i,t}, Steering_{i,t}) \tag{2.2}$$

We performed two types of feature from all driving variables and arousal as follows.

2.3.3.1 Statistical Features

These features include the mean and standard deviation of all driving variables of the past five seconds. These standard descriptive statistics exhibit the characteristics of the value distribution of each driving variables.

2.3.3.2 Correlative Features

We also computed the Pearson correlation between driving variables of five seconds before with the arousal of five seconds later. These features not only showed the mutual relationship between driving variables and human variables but also captured each driver's characteristics during their driving session. We later fed these features to a

clustering algorithm to discriminate between groups of drivers' characteristics. Figure 2.5 depicts two typical observed patterns of correlation between driving variables and human arousal. While $Subject\ \#07$ showed a substantial correlation between driving variables and the arousal, $Subject\ \#08$ showed no correlation.

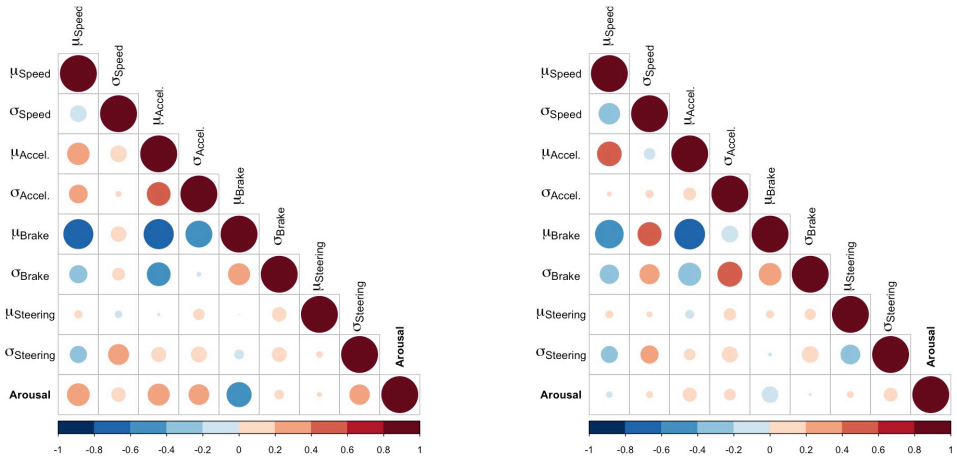

(A) Subject #07 (B) Subject #08

FIGURE 2.5: Two main patterns of correlation matrices.
Size of circles indicate the absolute value of correlation.

2.3.4 Linear Model

To analyze how much the arousal of all subjects varied as the driving variables varied, we constructed a cross-sectional linear model with random effects on subjects. In this model, the arousal was explained by driving variables (explanatory variables). Equation 2.3 shows the regression model that describes the arousal of subject i at time t in

the time window of 10 seconds.

$$\begin{aligned}\Delta\text{PP}_{\text{ORD}_{i,t+5}} = &\beta_{Speed_\mu}\mu_{Speed_{i,t}} + \beta_{Speed_\sigma}\sigma_{Speed_{i,t}} \\ &+ \beta_{Accel_\mu}\mu_{Accel_{i,t}} + \beta_{Accel_\sigma}\sigma_{Accel_{i,t}} \\ &+ \beta_{Brake_\mu}\mu_{Brake_{i,t}} + \beta_{Brake_\sigma}\sigma_{Brake_{i,t}} \\ &+ \beta_{Steering_\mu}\mu_{Steering_{i,t}} + \beta_{Steering_\sigma}\sigma_{Steering_{i,t}} \\ &+ \mu_i + \beta_o + \epsilon_{i,t}\end{aligned} \tag{2.3}$$

2.3.5 Hierarchical Clustering

To delve into the types of drivers and their associated relationship between driving variables and arousal, we used a clustering algorithm to discriminate between drivers into groups with similar characteristics. With a dataset that has a small number of observations like what we have in this study, hierarchical clustering is the method of choice (Baker and Hubert, 1975). Besides, the dendrogram of hierarchical clustering not only provided us intuitive visualizations, but also gave us a simple way to split or join clusters.

Agglomerative clustering and divisive clustering are two general strategies of hierarchical clustering. While agglomerative clustering is a bottom-up approach that initiates each driver as a cluster and continues to merge clusters, divisive clustering is a top-down approach that initiates all drivers as a single cluster and performs splitting recursively. A measure of dissimilarity between groups of drivers was required to decide which clusters should be combined or divided. The algorithm decided by using an appropriate metric of the distance between pairs of observations and a linkage criterion, which specifies the dissimilarity of sets as a function of the pairwise distances of observations in the sets. In this study, we chose Euclidean as a distance metric (Equation 2.4). To maximize the discrimination between clusters, we selected the complete linkage function (Defays, 1977) as the linkage criterion. Equation 2.5 expresses the complete linkage function, meaning the distance $D(X, Y)$ between clusters X and Y,

as:

$$d(x, y) = \|x - y\|_2 = \sqrt{\sum_i (x_i - y_i)^2} \tag{2.4}$$

$$D(X, Y) = \max_{x \in X, y \in Y} d(x, y) \tag{2.5}$$

where

- $d(x, y)$ is the distance between subjects $x \in X$ and $y \in Y$
- X and Y are two sets of subjects (clusters)

At this stage, we fed all correlative features into the clustering algorithm. Although standardizing these features on the same scale is recommended (Mohamad and Usman, 2013), it does not solve the problem and might lead to a change of the final structure (Kaufman, 2005). Providentially, all correlative features had a clear value range between -1 and 1. Therefore, standardizing these values was not necessary for our approach.

Besides, we used Silhouettes (Rousseeuw, 1987) to determine the optimal number of clusters. This method not only provides an interpretation and validation of consistency within clusters, but also provides a succinct graphical representation to evaluate the goodness of the structure.

2.3.6 Machine Learning Model

Because of robustness in overfitting, interpretability, and computational efficiency (Chen and Guestrin, 2016), we chose Extreme Gradient Boosting (XGBoost) to predict the drivers' arousal in the next five seconds. We classified each driver's average arousal in five seconds into two classes (low arousal and high arousal). To discriminate between the two classes and label data samples, we used the Otsu algorithm to determine a binary threshold (Otsu, 1979). Subsequently, we fed all statistical features of driving variables in the past five seconds into XGBoost models to predict the class of average

arousal in the next five seconds.

The XGBoost model constructs an ensemble of decision trees. At the training phase, multiple trees are formed sequentially in a stepwise manner, with each tree resolving the weaknesses or wrong predictions of the previous tree. When testing a new sample, each tree yields a probability score for each class, and a weighted combination gives the final estimate. This algorithm implements a gradient descent methodology to find the optimal structure of the trees. Equation 2.6 shows the formula of a prediction of the model in step t.

$$\hat{y}^t = \sum_{k=1}^{t} h_k(x) = \sum_{k=1}^{t-1} h_k(x) + h_t(x) = \hat{y}^{t-1} + h_t\left(x\right) \tag{2.6}$$

where $h_k(x)$ represents the function corresponding to the tree developed at step k,.

The optimization aim is to reduce the binary loss from the predictive value $\hat{y}^t$ to the actual value of y. This is shown as:

$$l\left(y, \hat{y}^t\right) = \sum_{i=1}^{n} \left(y_i \ln\left(1 + e^{-y_i^t}\right) + (1 - y_i) \ln\left(1 + e^{y_i^t}\right)\right. \tag{2.7}$$

where y_i is the actual value of observation i in a total of N observations.

2.4 Results

2.4.1 Linear Model

Table 2.1 shows a summary of the linear model with random effects. According to this result, we can see the overall effects of driving variables on all drivers. As the beta coefficient estimate of the standard deviation of speed β_{V_2} is positive, the change of speed shows a positive trend with respect to drivers' arousal. Seconds, the negative value of the coefficient estimate of the mean of brake force indicates the decrease of arousal as drivers stop at crossroads.

TABLE 2.1: Summary of the linear model with random effects to predict arousal in the next five seconds on data of the On-road Driving study.

Coefficient	Estimate	Std. Error	df	t value	Pr(>|t|)	
β_{Speed_μ}	0.00029	0.00016	1879.42228	1.84304	0.06548	
β_{Speed_σ}	0.00500	0.00158	1879.35200	3.15687	0.00162	**
β_{Accel_μ}	-0.00021	0.00072	1880.18525	-0.28717	0.77401	
β_{Accel_σ}	0.00089	0.00154	1880.32728	0.57475	0.56553	
β_{Brake_μ}	-0.00202	0.00049	1880.53147	-4.13182	0.00004	***
β_{Brake_σ}	0.00226	0.00090	1879.09356	2.51553	0.01197	
$\beta_{Steering_\mu}$	0.00033	0.00014	1879.88145	2.36431	0.01816	
$\beta_{Steering_\sigma}$	-0.00012	0.00026	1879.09798	-0.48026	0.63110	
β_o	0.21907	0.06214	10.19210	3.52550	0.00533	**

2.4.2 Clustering - Types of Drivers

Table 2.2 presents the two groups of drivers based on clustering the correlative features of driving variables of the past five seconds with the driver's arousal in the next five seconds. While drivers in the group C_1 stay calm and have no correlation with driving variables, drivers' arousal in the group C_2 shows notable positive trends with accelerating and braking. Besides, drivers in the group C_2 also show negative trends with respect to braking. The dendrogram of Figure 2.6(A) visualizes these two separate groups of drivers.

TABLE 2.2: Clustering result of the correlative features between driving variables and drivers' arousal with a 5-5 seconds time window.
Red text and arrow show positive trends, while blue text and arrows show negative trends.

Subj.	μ_{Speed}	σ_{Speed}	$\mu_{Accel.}$	$\sigma_{Accel.}$	μ_{Brake}	σ_{Brake}	$\mu_{Steer.}$	$\sigma_{Steer.}$	**Group**
#01	0.162	-0.06	0.019	0.047	-0.066	-0.098	↑0.227	↓-0.314	C_2
#04	0.011	-0.013	-0.002	0.123	-0.137	0.136	-0.103	↑0.218	C_2
#05	↑0.306	0.182	↑0.346	↑0.273	↓-0.362	0.163	↑0.231	↑0.281	C_1
#06	0.152	0.078	↑0.306	↑0.238	↓-0.363	0.054	-0.007	0.132	C_1
#07	↑0.370	0.143	↑0.348	↑0.307	↓-0.454	0.059	0.015	↑0.297	C_1
#08	-0.025	0.028	0.136	0.091	-0.192	0.003	0.027	0.13	C_2
#10	↓-0.319	0.105	-0.072	-0.006	0.146	0.141	0.007	0.141	C_2
#11	↑0.306	0.108	↑0.280	0.121	↓-0.284	0.025	0.042	0.164	C_1

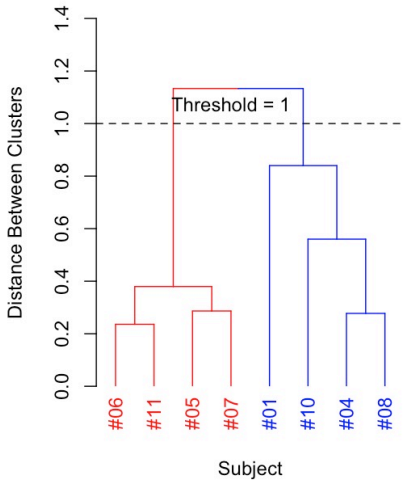

FIGURE 2.6: Clustering result of 5-5 seconds time window

2.4.2.1 Accelerophobic Drivers

We named drivers in the group C_1 $accelerophobic\ drivers$ based on their arousal responses to acceleration and braking. Figure 2.7 depicts the correlation between all driving variables and arousal in Subject $\#06$.

According to Figure 2.7, at the entrance and exit of the highway, annotated with circles [A][B], their arousal increased when speed and acceleration increased or reduced. Oppositely, their arousal dropped while waiting for the traffic light at intersections such as [D] where drivers stop fully. This observation was more noticeable with respect to non-stop intersections such as [C], where the vehicles crossed intersections without stopping. According to Table 2.2, this driver's arousal had positive trends in relation to the change of acceleration, meaning similar to other accelerophobic drivers. However, their response to speed is different. For instance, this driver stayed calm when driving at [60-70] mph on the highway [E]. Although a small number of subjects do not sufficiently represent the whole population, this phenomenon still indicates that speed is not always the main factor but acceleration.

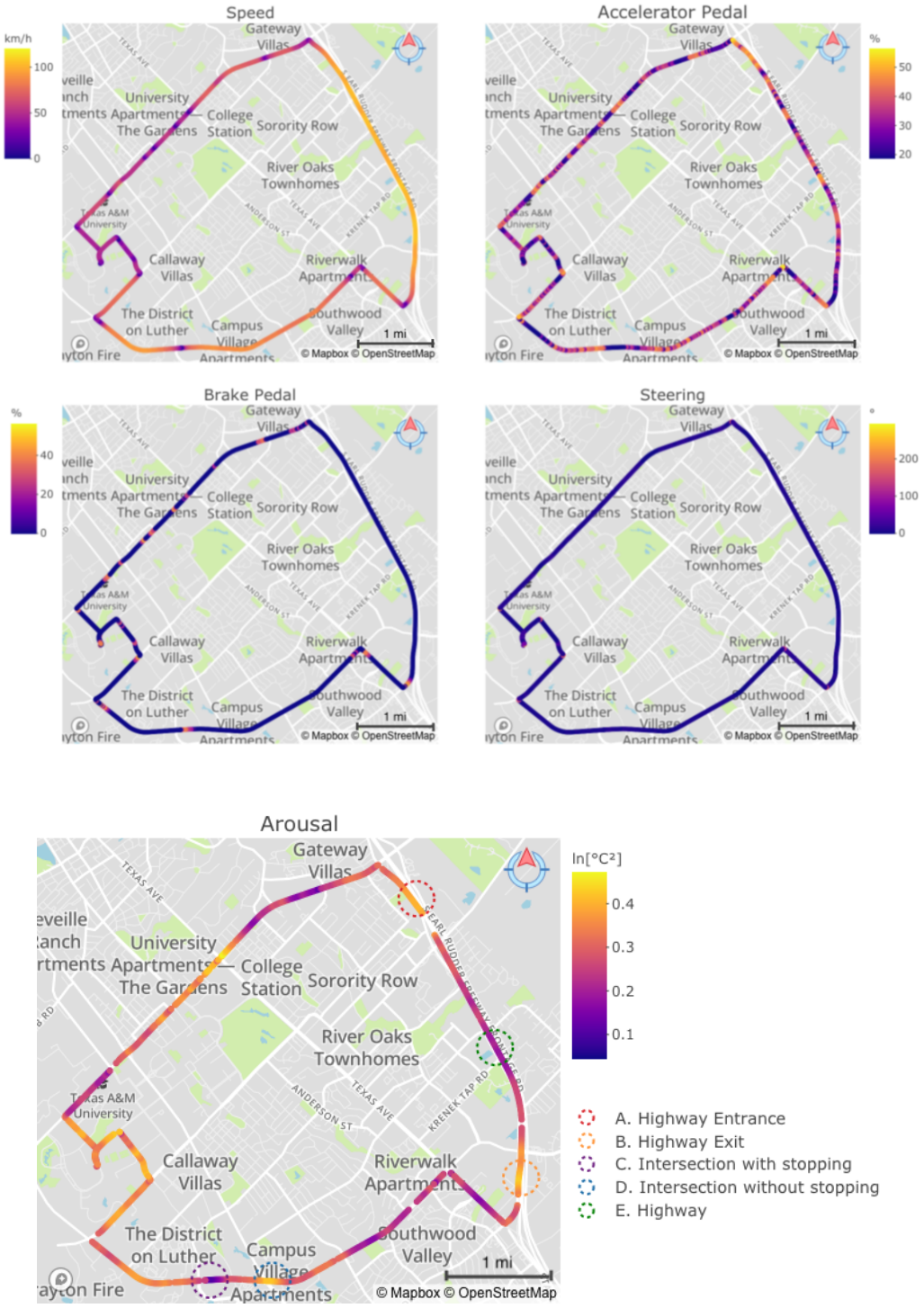

FIGURE 2.7: Visualization of the full itinerary and the association between driving variables and arousal.
The discontinuous line of arousal is due to technical issues with capturing thermal images or to difficulties extracting perinasal perspiration when drivers moved their face too quickly. Dotted circles in the arousal plot indicate locations with interesting observations.

2.4.2.2 Sensitivity Analysis

We also performed a sensitivity analysis by applying the clustering algorithm on different time windows of five, 10, 15, and 30 seconds of driving variables. Figure 2.8 shows no change in the members of each cluster. With a small variance of the threshold value of the distance between clusters, the subjects remained consistently in two separate groups. The hierarchical structure of drivers remained consistently with time windows from five to 15 seconds. There was a minor internal change in one cluster during the 30-second time window.

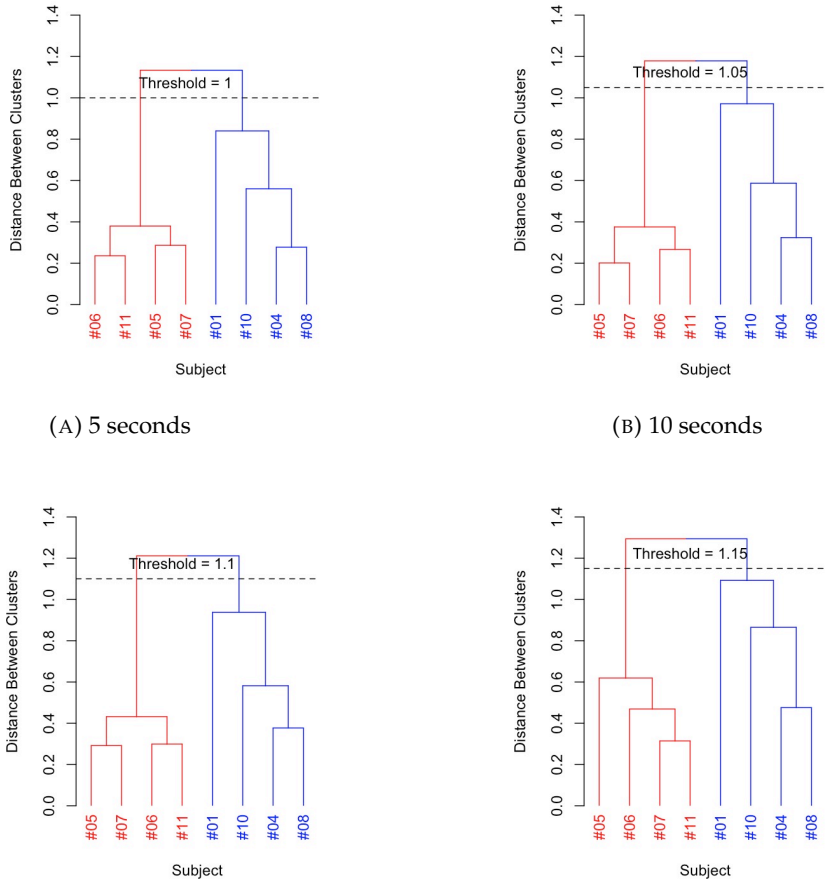

(A) 5 seconds

(B) 10 seconds

(C) 15 seconds

(D) 30 seconds

FIGURE 2.8: Hierarchical clustering of types of drivers with different time windows of 5, 10, 15, and 30 seconds.
The red branch includes accelerophobic drivers who were sensitive to the change in acceleration. The blue branch consists of remaining subjects who showed minor or no association.

2.4.3 Predicting Arousal from Driving Variables

We performed five-fold stratified cross-validation (Stone, 1974) to evaluate the effectiveness of the online model predicting trends of arousal in the next five seconds. Accordingly, the original sample was randomly partitioned into five equal-sized subsamples with a stratified strategy. The XGBoost algorithm used four subsamples for training and retained one subsample for testing. This process was repeated five times with a different subsample used for testing each time. The mean and standard deviation of performance metrics were performed at the end of this process.

Table 2.3 shows the performance metrics of XGBoost short-term prediction model for each subject.

TABLE 2.3: Performance of ML model training and testing on data of each subject

Subject	Accuracy	Precision	Recall	Spec	F1	NPV	AUC
Subject #01	0.92	0.85	0.84	0.95	0.85	0.94	0.97
Subject #04	0.89	0.88	0.83	0.93	0.85	0.90	0.96
Subject #05	0.90	0.91	0.90	0.90	0.91	0.89	0.96
Subject #06	0.90	0.94	0.90	0.89	0.92	0.83	0.96
Subject #07	0.92	0.94	0.92	0.92	0.93	0.88	0.97
Subject #08	0.90	0.92	0.89	0.90	0.91	0.86	0.96
Subject #10	0.93	0.96	0.94	0.92	0.95	0.88	0.98
Subject #11	0.92	0.97	0.93	0.89	0.95	0.79	0.97

Chapter 3

Test Track Driving 1 Study

3.1 Study Design

3.1.1 Subjects

The study took place at the test track facility of Texas A&M University. It included 33 subjects aged between 18 and 72 years old. From the 33 subjects that participated in the study, we acquired usable data for 21 subjects (63.636%), including 11 males (52.381%) and 10 females (47.619%). The other 12 subjects did not have full recorded data to develop our model.

3.1.2 Experimental Setup

During the experimental sessions of this study, the systems continuously imaged the participants' faces with a thermal and visual camera. In general, the experimental setup in the car of this study was similar to the ORD study. The systems also captured participants' physiological signals with a wearable device. Detailed descriptions of each system are as follows.

3.1.2.1 Sensors for Human

- *Thermal facial camera.* We used a Tau 640 long-wave infrared (LWIR) camera (FLIR Commercial Systems, Goleta, CA); it features a small size $(44 \times 44 \times 30\ \mathrm{mm})$ and adequate thermal $(< 50\ \mathrm{mK})$ and spatial resolution $(640 \times 512$ pixels). The 640

camera was outfitted with an LWIR $35\ \mathrm{mm}$ lens $f/1.2$. Thermal data was collected at a frame rate of 7.5 fps. We used these thermal facial videos to extract perinasal perspiration signals, known to commensurate with electrodermal (EDA) activity in the palm. For this reason, we call the thermally extracted perinasal perspiration signals, *perinasal EDA signals*.

- *Visual facial camera.* A Logitech HD Pro - C920 camera (Logitech, Newark, CA) with spatial resolution 1920×1080 pixels and a frame rate of 30 fps. It is placed $1\ \mathrm{m}$ from drivers, tucked atop driver's side car dashboard (Figure 2.1). The appropriate distance in combination with the camera optics ensured that a typical face covered a significant portion of each thermal and visual frame, providing maximum spatial resolution for image analysis.

- *Visual dash camera.* This camera was placed on the car dash, aiming at the front view of the car, to record the subject's drive. We use a Logitech Brio camera (Logitech, Newark, CA) with spatial resolution 1280×720 pixels and a frame rate of 30 fps.

We collected additional physiological data via a wearable sensors.

- *Adrenergic sensor.* We used the Zephyr BioHarness 3.0 (Zephyr Technology, Annapolis, MD) sensor to measure the subject's heart rate and breathing rate-two standard indicators of adrenergic control. The sensor connects to a chest strap that is worn underneath the subject's clothing. It is powered by a rechargeable lithium polymer battery (up to $26\ \mathrm{h}$ per charge) and is capable of detecting a heart rate range of $25 - 240$ bpm and a breathing rate range of $4 - 70$ bpm.

3.1.2.2 Sensors for Vehicle

Similarly, we also used a Dewetron Data Acquisition System to record and save driving variables. These variables included speed, acceleration, brake force, steering angle, and lane position.

3.1.3 Experimental Design

Upon signing the consent form, the subjects completed questionnaires that identified key facts about the subject, including gender and age. Subsequently, subjects in the TTD1 study performed four drives in the driving facility under different types of stressor s. The detailed design of the four drives are as follows:

- *Normal Drive (ND).* Driving the vehicle in the absence of a stressor ($s = N$).
- *Cognitive Drive (CD).* Driving the vehicle under a cognitive stressor ($s = C$): Subjects were asked to subtract by 13, sequentially starting from 1,022. When they gave a wrong answer, they were stopped and asked to restart subtractions from 1,022.
- *Motoric Drive (MD).* Driving the vehicle under a motoric stressor ($s = M$): Subjects had to text back words that appeared sequentially on the screen of a smartphone.
- *Failure Drive (FD).* The subjects were split into three groups based on the type of the applicable stressor s: no stressor ($G_{FD_{s=N}}$), cognitive ($G_{FD_{s=C}}$), and motoric ($G_{FD_{s=M}}$). Near the end of this drive, all the subjects experienced an unintended acceleration to simulate a *catastrophic event* E_{FD}.

In ND, CD, and MD drives, these subjects had to drive a one-mile runway four times, performing four U-turns. For each subject, the order of these three drives was randomized; then, there are 3! = 6 possible permutations, as follows:

$$ND - CD - MD, \;\; ND - MD - CD, \;\; CD - ND - MD$$

$$CD - MD - ND, \;\; MD - ND - CD, \;\; MD - CD - ND$$

Table B.1 shows the randomized order of experiments in the first three experiments.

In the last Failure Drive (FD), these subjects drove on the straight runway only once. For this drive, the subjects were split into three groups, depending on what type of one of the three applicable stressors, as mentioned earlier. This drive consisted of two phases, as follows:

- *Phase* $P1_{FD_{i,s}}$. At the beginning of FD, the subject i experienced the same type of stressor s that they had experienced in their first experimental drive.
- *Phase* $P2_{FD_{i,s}}$. At the end of the runway, after driving under the stressor s in Phase $P1_{FD_{i,s}}$, the subject i experienced an unintended acceleration event, simulating a catastrophic event E_{FD}.

For all drives, the speed limit was set at $30\ \mathrm{mph}$. The experimenter advised the subjects when their speed was falling outside the required range [25, 35] mph so that they increased or decreased their speed accordingly.

3.1.4 Signal Extraction

At this step, we performed similar steps *Tissue tracking & perinasal perspiration signal extraction* and *Driving Data Extraction* as in On-road driving study.

3.1.4.1 Tissue Tracking and Perinasal Perspiration Signal Extraction

We used a tissue tracker reported by Zhou et al. (Zhou et al., 2013). Initially, we initiated the tracking algorithm by selecting the subject's perinasal region in the first frame. In every subsequent frame, the tracker determined the best matching section of the thermal clip via spatiotemporal smoothing. In the selected and matching region of the thermal images, activated perspiration pores appeared as "cold" (dark) spots, amidst "hot" surrounding tissue (Figure 2.2). Finally, to compute the perspiration signal, we applied a morphology-based algorithm to the measurement region of interest (MROI) (Shastri et al., 2012).

3.1.4.2 Driving Data Extraction

All incoming driving signals were filed in a single database. These included speed, acceleration, brake force, steering angle, pulse-per-second (PPS) signal of a GPS satellite, and time-related information. We used Dewesoft, a data acquisition software, to extract tabular data from the database.

3.2 Database

We publicly hosted quantitative data and videos of Test Track Driving 1 study on a Open Science repository at *https://osf.io/974vf/*.

3.2.1 Quantitative Data

The quantitative data folder holds comma separated value (csv) files for each subject. In the data summary file, in addition to the columns showing the Time value (Column A), there are columns holding physiological data (Columns B), columns holding vehicle variables (Columns D - I and M), and columns holding information about the drive (Columns B and J-L).

- $ColumnB : Perspiration$: Values of the perinasal perspiration signal in $^{\circ}C^{2}$.
- $ColumnC : Drive$: Type of drive
  - ➔ 1 ≡ Normal drive (no stressor)
  - ➔ 2 ≡ Cognitive stressor drive
  - ➔ 3 ≡ Motoric stressor drive
  - ➔ 4 ≡ Failure drive (either no stressor, Cognitive stressor, or Motoric stressor, and an unintended acceleration event at the end)
- $ColumnD : Speed$: Speed in mph. Speed limit is 30 mph.
- $ColumnE : Acceleration$: Accelerator pedal force in %.

- $ColumnF$: $Braking$: Brake pedal force in %.
- $ColumnG$: $Steering$: Steering angle in °.
- $ColumnH$: $LaneDeviation$: Center of the vehicle with respect to the middle of the lane.
- $ColumnI$: $Distance$: Distance in meters from the starting pylon.
- $ColumnJ$: $Activity$: Type of activity in the drive
  - ➔ 0 ≡ U-turn
  - ➔ 1 ≡ Normal
  - ➔ 2 ≡ Cognitive
  - ➔ 3 ≡ Motoric
- $ColumnK$: $Failure$: Indicator of unintended acceleration
  - ➔ 0 ≡ no unintended acceleration
  - ➔ 1 ≡ unintended acceleration present
- $ColumnL$: $Phase$: Phase of the drive
  - ➔ 0 ≡ U-turn segment of the drive
  - ➔ 1 ≡ P1: 1st straight segment of the drive
  - ➔ 2 ≡ P2: 2nd straight segment of the drive
  - ➔ 3 ≡ P3: 3rd straight segment of the drive
  - ➔ 4 ≡ P4: 4th straight segment of the drive
- $ColumnM$: $NewSteering$: New value of steering angle.

3.3 Methods

3.3.1 Methodological Flow

Our primary goal of using data in this study was to test the persistence of arousal changes of accelerophobic drivers that we found in the ORD study. Accordingly, we used the associated subjects' arousal after different acceleration levels in everyday drives, such as ND, CD, and MD drives, to predict their arousal at the catastrophic event E_{FD} in FD drive. While the online prediction model built on data from the ORD study produces short-term predictions of trends in arousal in the next five seconds, the predictions made by the predicting model in this study can be considered to be more long-term. Figure 3.1 depicts the methodological flow of our approach. In this approach, we used all arousal of perinasal perspiration signals and stressors that drivers experience as variables. After preprocessing the variables and extracting features, we built a linear model to see the overall association between the drivers' arousal in normal driving with their arousal at the simulated catastrophic event. Subsequently, we built a machine learning model to predict the trend of arousal at the catastrophic event. The remainder of this section details the individual elements of the flow.

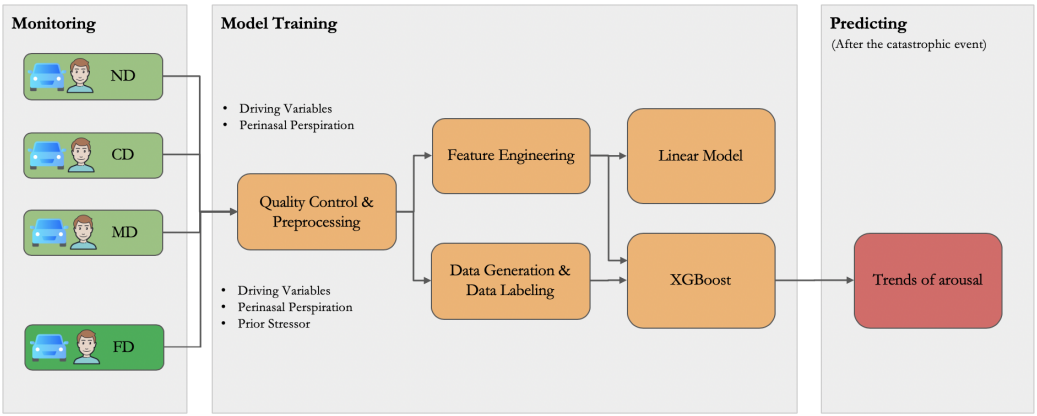

FIGURE 3.1: Overview of methodological flow of our approach on Test Track Driving 1 study

3.3.2 Preprocessing and Quality Control

For each drive in this study, we applied data validation and performed noise removal, data resampling, and normalization on perinasal perspiration like what we did with data in ORD study. For perinasal perspiration normalization, we used the mean of perspiration in runways of ND drive as the baseline perspiration of each subject. Therefore the arousal ($\Delta PP_{d_{it}}$) of subject i in drive d at time t is defined as:

$$\Delta PP_{d_{it}} = ln(PP_{d_{it}}) - ln(\mu_{PP_{ND_i}}) \tag{3.1}$$

3.3.3 Feature Engineering

As in the ORD study, we used a time window to extract driving variables and perspiration. As the speed limit in this study was controlled and was much less than that of the ORD study, we used 3-3 seconds as the time window instead of 5-5 seconds time window. Accordingly, we computed standard statistics for driving parameters of the last three seconds and the mean of arousal of the next three seconds.

In the next step, we applied the definition of accelerophobic drivers that we found in the ORD study to extract associated features. From the statistics of driving variables, we partitioned samples of arousal into two parts based on acceleration levels. When driving, subjects' acceleration takes one of two modes. Therefore, we used the Otsu algorithm for each subject's acceleration distribution in each drive to determine a threshold to partition the data. Finally, we had two sets of arousal samples, as follows:

- $\Delta\text{PP}_{d_{i,t,\text{LA}}}$: Means of three seconds of arousal of subject i in drive d after a low acceleration (LA) at time t.
- $\Delta\text{PP}_{d_{i,t,\text{HA}}}$: Means of three seconds of arousal of subject i in drive d after a high acceleration (HA) at time t.

3.3.4 Data Generation and Data Labelling

To build a classification machine learning model to predict arousal trends after the catastrophic event, we generated more data sampled from the original data set and labeled the data sample based on the changing levels of arousal.

3.3.4.1 Data Generation

Full extracted data from 21 subjects is a too small number of samples for building a robust predicting machine learning model. Therefore, we had to generate more samples from the original data set. As mentioned earlier, these subjects drove in four segments in each drive. Each segment included driving along the runway and a U-turning. We assumed each time or a pair of driving along the runway and U-turning as a separate drive. Accordingly we split each original drive into four generated drives and extract features separately from these drives. Finally, we produced 84 samples from 21 original samples.

3.3.4.2 Data Labelling

From the distribution of arousal of all subjects at the simulated catastrophic event, we noticed there were two levels of increasing of arousal. While one group showed no change in arousal after a catastrophic event, the other group exhibited a notable arousal increase in arousal. We named the former the normal group ($Group_{\text{False}}$) and the latter the accelerophobic ($Group_{\text{True}}$). To separate the two groups, we also used the Otsu algorithm (Otsu, 1979) to determine a threshold to split the two classes. From this we obtained nine subjects in $Group_{\text{True}}$ and remained 11 subjects in $Group_{\text{False}}$.

3.3.5 Linear Model

We built a linear model expressing the arousal of subject i at the catastrophic event after driving under stressor s in Failure Drive, denoted as ($\Delta PP_{P2_{FD,i,s}}$), from values of their arousal after low and high accelerations in Cognitive Drive and Motoric Drive.

Equation 3.2 expresses this cross-sectional regression model as

$$\begin{aligned}\Delta\text{PP}_{\text{P2}_{\text{FD},i,s}} = {} & \beta_{\text{CD}_{\text{HA}}}\mu\Delta\text{PP}_{\text{CD}_{\text{HA},i}} + \beta_{\text{CD}_{\text{LA}}}\mu\Delta\text{PP}_{\text{CD}_{\text{LA},i}} \\ & + \beta_{\text{MD}_{\text{HA}}}\mu\Delta\text{PP}_{\text{MD}_{\text{HA}},i} + \beta_{\text{MD}_{\text{LA}}}\mu\Delta\text{PP}_{\text{MD}_{\text{LA},i}} \\ & + D(s) + \beta_o + \epsilon_i\end{aligned} \tag{3.2}$$

3.3.6 Machine Learning Model

We also used the XGBoost algorithm (Chen and Guestrin, 2016) to build a predicting model with an ensemble of decision trees. This model used the features extracted according to the definition of the accelerophobic drivers in the ORD to predict the expected response of their arousal after the simulated catastrophic event.

3.4 Results

3.4.1 Linear Model

Table 3.1 shows a summary of the linear model. According to the values of coefficients, we can see the overall effects of arousal after high and low accelerations in normal drives on driver's arousal after the simulated catastrophic event in the Failure Drive. The number of asterisks indicates the level of significance: **: p-value $\leq$ 0.01, ***: p-value $\leq$ 0.001. The positive regression coefficients of arousal after high accelerations, $\beta_{CD_{HA}} = 2.11765$, and $\beta_{MD_{HA}} = 2.97984$, express a strong positive effect on arousal right after the catastrophic event. Besides, the type of stressor also has an impact on the outcome of the final arousal. Both cognitive and motoric stressors have positive coefficients, $D_{s=C} = 0.17285$ and $D_{s=M} = 0.16446$.

Figure 3.2 depicts the association of arousal after high accelerations in the Cognitive Drive and the Motoric Drive with the arousal after the catastrophic event in the Failure Drive. In this figure, accelerophobic drivers, including Subject #01, Subject #06, and

TABLE 3.1: Summary of the cross-sectional linear model to predict drivers' arousal at catastrophic event on the Test Track Driving 1 study

Coefficient	Estimate	Std. Error	t value	Pr(>|t|)	
$\beta_{\text{CD}_{\text{HA}}}$	2.11765	0.65809	3.21788	0.00620	**
$\beta_{\text{CD}_{\text{LA}}}$	-1.58805	0.65839	-2.41204	0.03016	
$\beta_{\text{MD}_{\text{HA}}}$	2.97984	0.73529	4.05262	0.00119	**
$\beta_{\text{MD}_{\text{LA}}}$	-2.53203	0.69956	-3.61948	0.00279	**
$D_{s=\text{C}}$	0.17285	0.05284	3.27108	0.00557	**
$D_{s=\text{M}}$	0.16446	0.04579	3.59153	0.00295	**
β_o	-0.21802	0.06604	-3.30124	0.00525	**

Subject #07, exhibited a strong arousal response across the board.

According to the linear model, we observed that arousal in daily drives can predict arousal in sudden unexpected acceleration events . Besides, the distraction at the time of incidents also have strong impacts on the arousal.

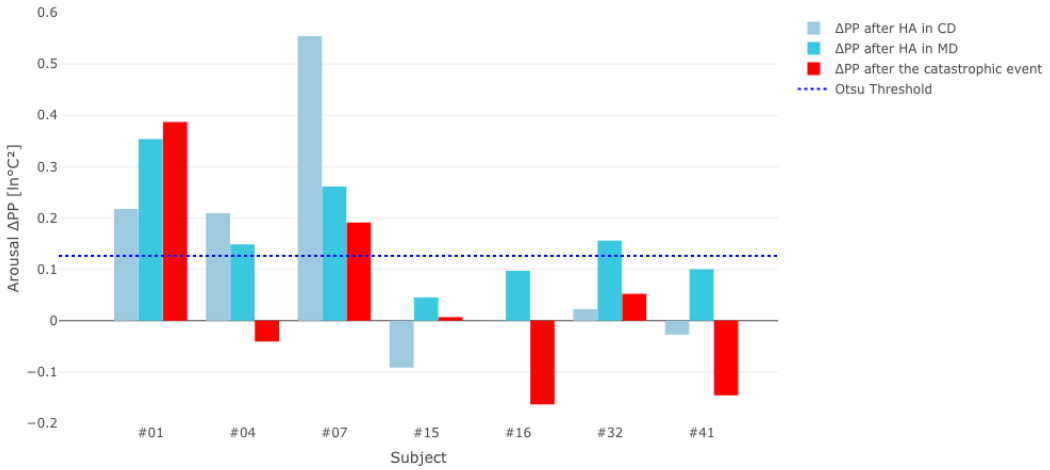

(A) G_N

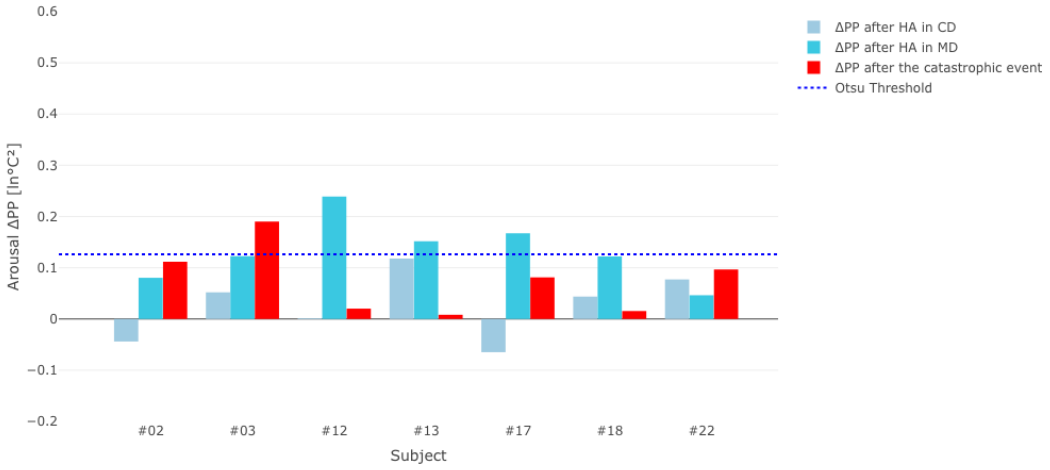

(B) G_C

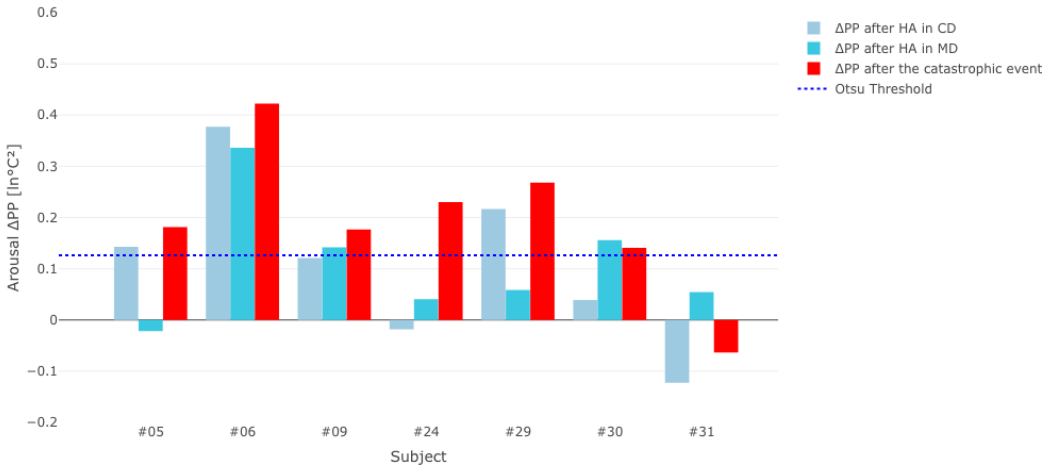

(C) G_M

FIGURE 3.2: Bar plots of the means of arousal of each subject after high accelerations (HA) in Cognitive Drive (CD), Motoric Drive (MD), and unintended acceleration in Failure Drive (FD).
The hyphenated lines indicate the Otsu threshold to separate the two classes of arousal after the catastrophic event. (A)(B) and (C) are three groups of subjects experiencing three different types of stressor in the FD, including no stressor, cognitive stressors and motoric stressors.

3.4.2 Machine Learning Model

We perform five-fold stratified cross-validation (Stone, 1974) to evaluate the effectiveness of this model for predicting trends of arousal. Table 3.2 shows the performance metrics of XGBoost prediction model.

TABLE 3.2: Performance of ML model

$Class_{High}$	$Class_{Low}$	Accuracy	Precision	Recall	Spec	NPV	F1	AUC
36	48	0.81	0.7	0.84	0.80	0.90	0.76	0.90

Chapter 4

Conclusion

4.1 Accelerophobia

This research produced a clustering model to discriminate between types of drivers based on the effect of driving variables on the driver stress as indicated by the changes in drivers' arousal. From the analysis of the effect, this works proposed two prediction models. One online predicting model produced arousal trends in the next five seconds based on driving variables in the last five seconds. The other long-term model used drivers' arousal during regular drives to predict those drivers' stress during and after a simulated catastrophic event.

From the clustering model in the ORD study, we found a group of "accelerophobic" drivers who shows a fear of acceleration but not of speed. In the TTD1 study, accelerophobic drivers exhibited strong arousal across the board. Their arousal after high accelerations in regular driving events was strongly associated with their arousal during and after the simulated catastrophic event.

Our proposed method can be practically applied through detection systems or accelerophobia tests. Car automation systems of future semi-automated or automated vehicles may be able to adjust the driving variables and control car safety module accordingly to the types of drivers. Especially for accelerophobic drivers, auto manufacturers may be able to find an optimal acceleration pattern and implement personalized car settings to

help them drive comfortably. In terms of the modification of cars (Stefano, Stuckey, and Kinsman, 2019) for people with disabilities, recognizing accelerophobia may help them avoid accidents or provide automated intervention in the case of unexpected events. By detecting the accelerophobia and its associated risk levels in each driver, insurance companies may be able to adjust the insurance rates accordingly. This method could also be used to provide tests to students in driving training schools. From the outcome of the test, schools could then guide those students and help them to avoid human errors that might lead to car accidents in the future.

4.2 Limitation and Future Research Plan

Although linear models and machine learning models in the two studies show significant results, there are limitations of data and methodology. Firstly, the number of subjects in both studies is still small. This observed phenomenon might happen with a small set of data but might not be present in large data sets. Secondly, there is a lack of incorporation with other physiological signals such as heart rate, breath rate, and psychometrics. Therefore, our plan for future research is to examine this method in relation to a large set of data and to incorporate other physiological signals and psychometrics.

Appendix A

On-road Driving Study

A.1 Noise Removal

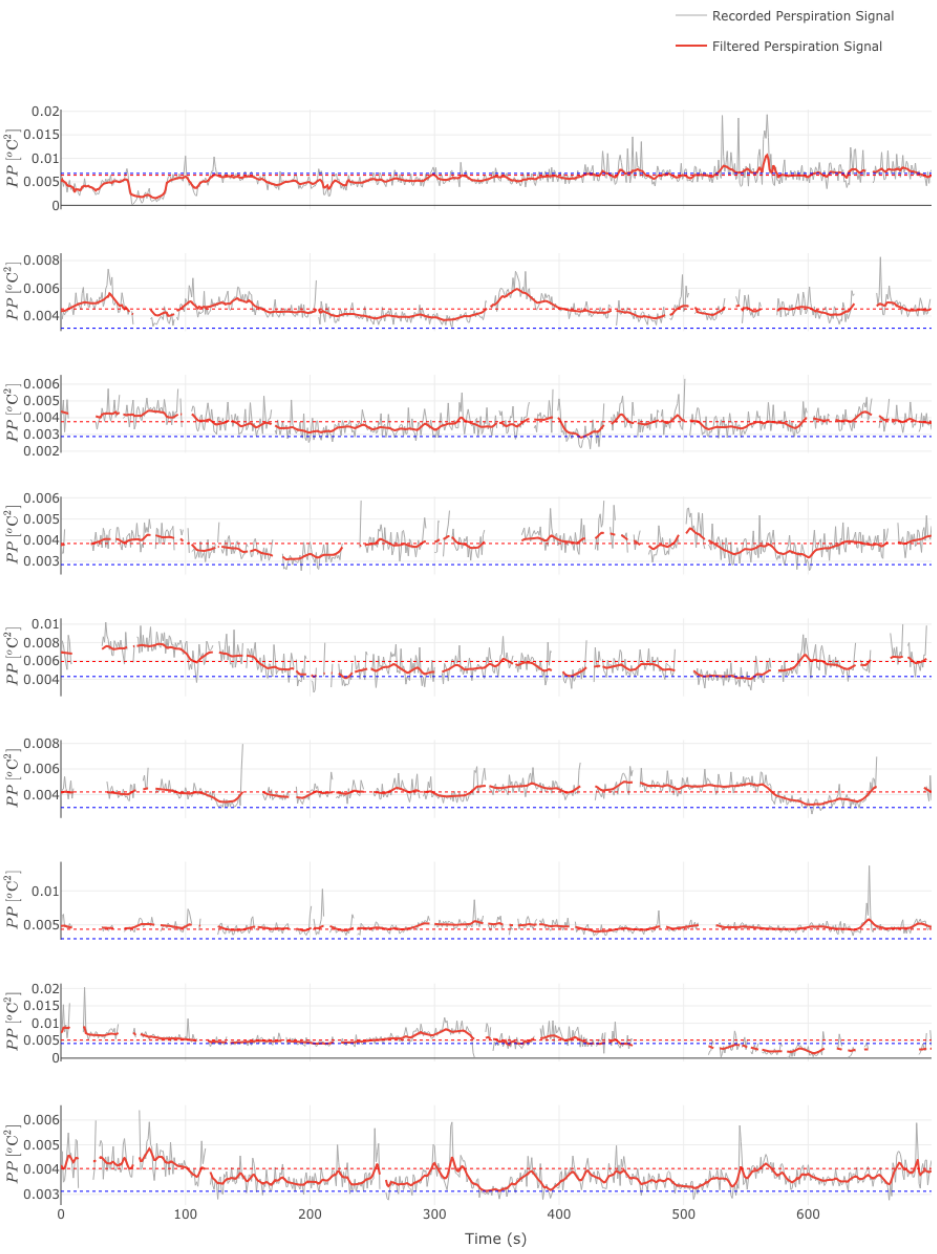

FIGURE A.1: Original recorded and noise-removed perinasal perspiration of all subjects.

Blue hyphenated lines indicate the mean of perspiration in the baseline session (BL). Red hyphenated lines indicate the mean of perspiration in the On-road driving session (ORD).

A.2 Correlation Matrices

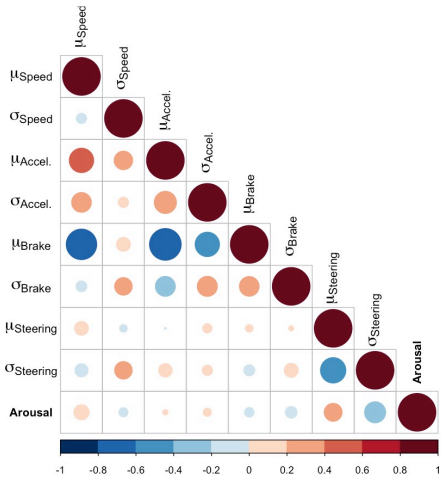

(A) Subject #01

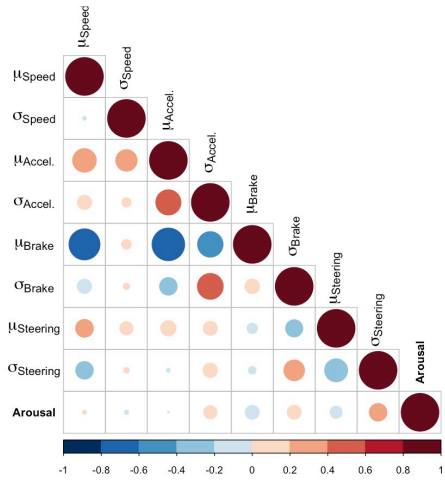

(B) Subject #04

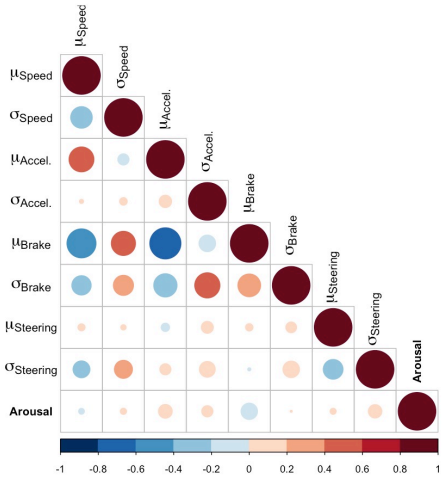

(C) Subject #08

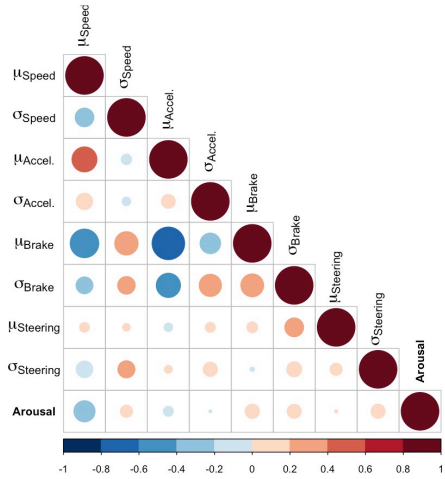

(D) Subject #10

FIGURE A.2: Correlation matrices of Normal Drivers.

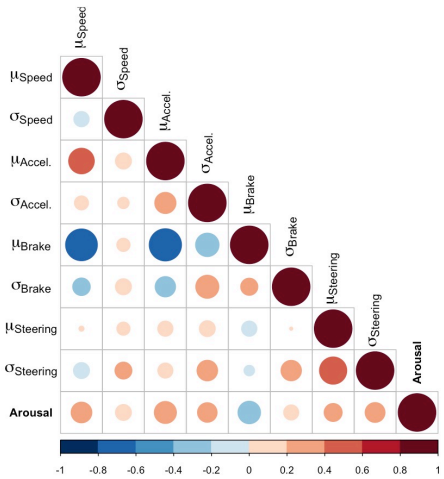

(A) Subject #05

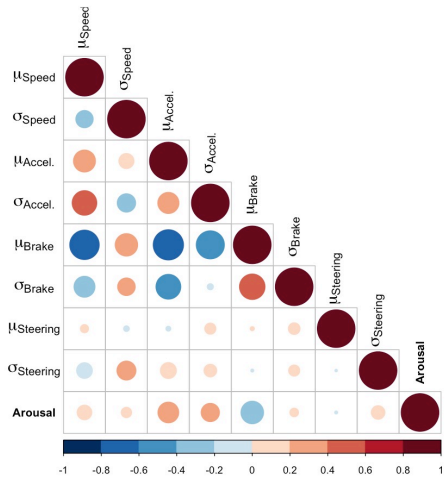

(B) Subject #06

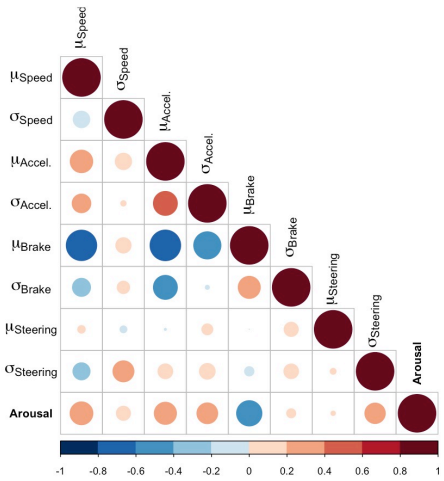

(C) Subject #07

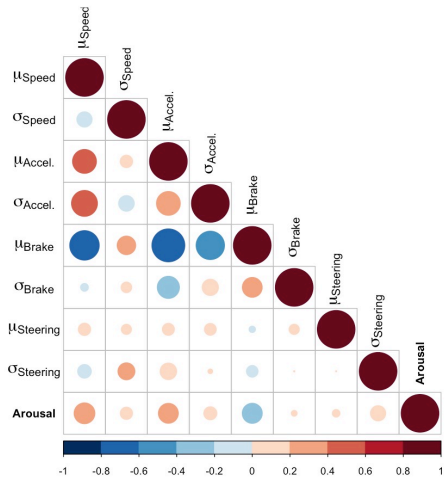

(D) Subject #11

FIGURE A.3: Correlation matrices Acclerophobic Drivers.

Appendix B

Test Track Driving 1 Study

B.1 Randomized Order of Experiments

TABLE B.1: Demography and order of experiments of all subjects

Subject	Age	Gender	1^{st} Drive	2^{nd} Drive	3^{rd} Drive	4^{th} Drive
T001	69	F	N	M	C	N
T002	23	M	C	N	M	C
T003	75	F	C	M	N	C
T004	22	F	N	M	C	N
T005	65	F	M	N	C	M
T006	70	M	M	C	N	M
T007	64	M	N	M	C	N
T009	18	M	M	N	C	M
T012	22	M	C	M	N	C
T013	85	M	C	N	M	C
T015	22	M	N	M	C	N
T016	60	F	N	C	M	N
T017	25	F	C	M	N	C
T018	72	M	C	M	N	C
T022	22	F	C	N	M	C
T024	61	F	M	C	N	M
T026	23	F	N	C	M	N
T029	22	F	N	M	C	N
T030	24	F	M	C	N	M
T031	24	M	M	N	C	M
T032	24	M	N	C	M	N
T041	71	M	N	C	M	N

B.2 Failure Drive (FD)

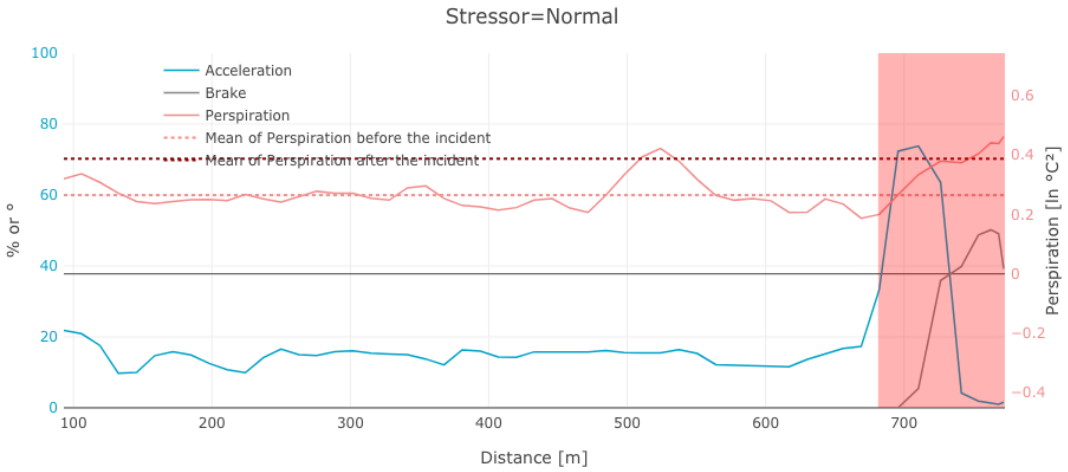

FIGURE B.1: Failure Drive of Subject #01

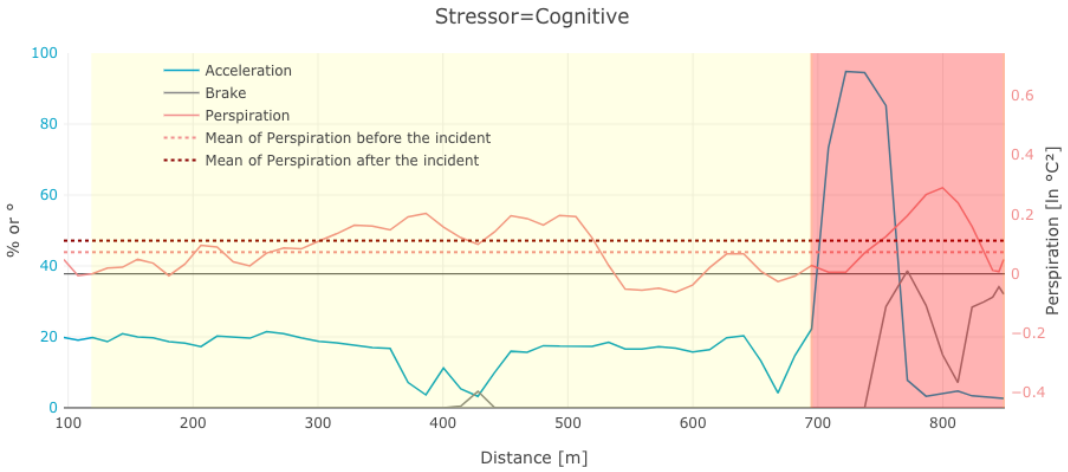

FIGURE B.2: Failure Drive of Subject #02

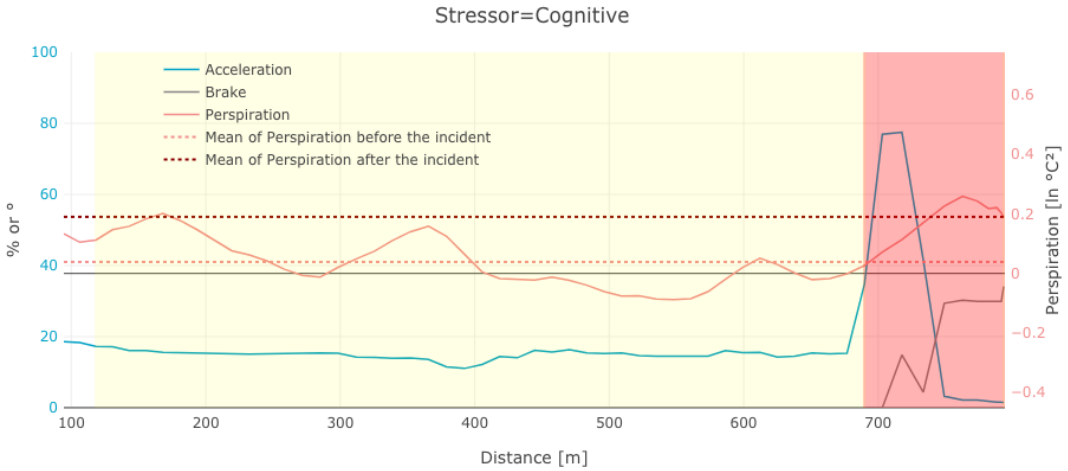

FIGURE B.3: Failure Drive of Subject #03

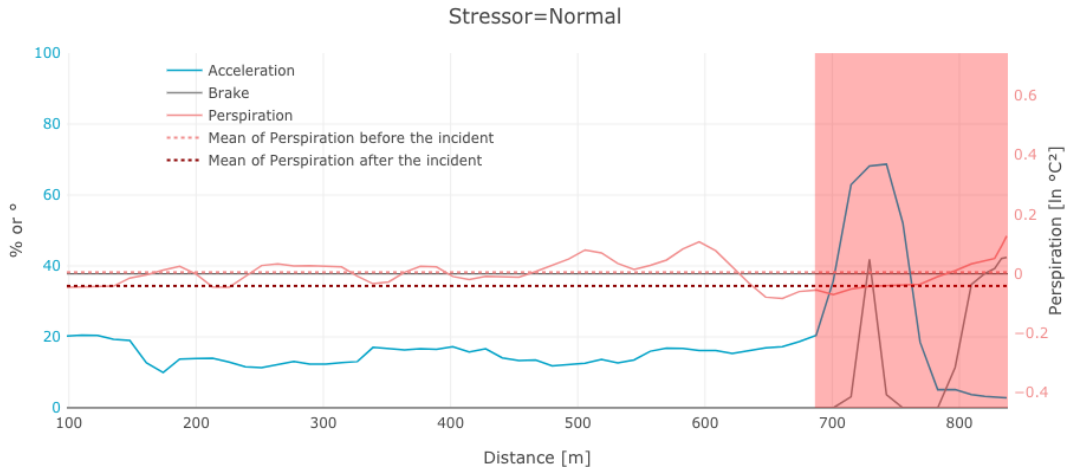

FIGURE B.4: Failure Drive of Subject #04

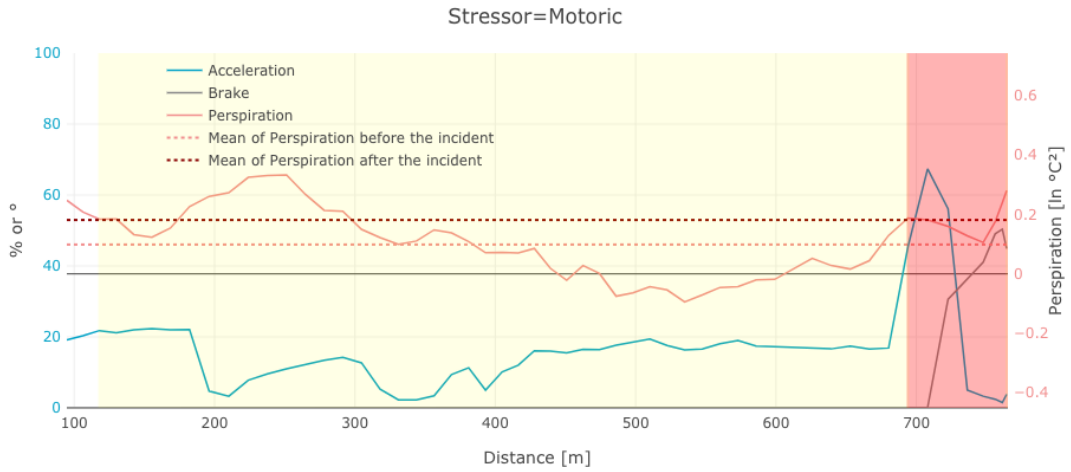

FIGURE B.5: Failure Drive of Subject #05

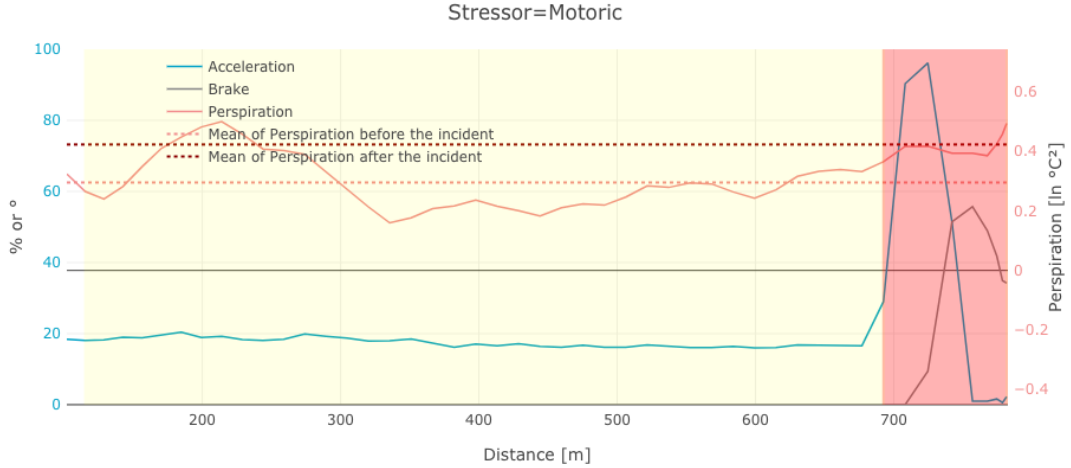

FIGURE B.6: Failure Drive of Subject #06

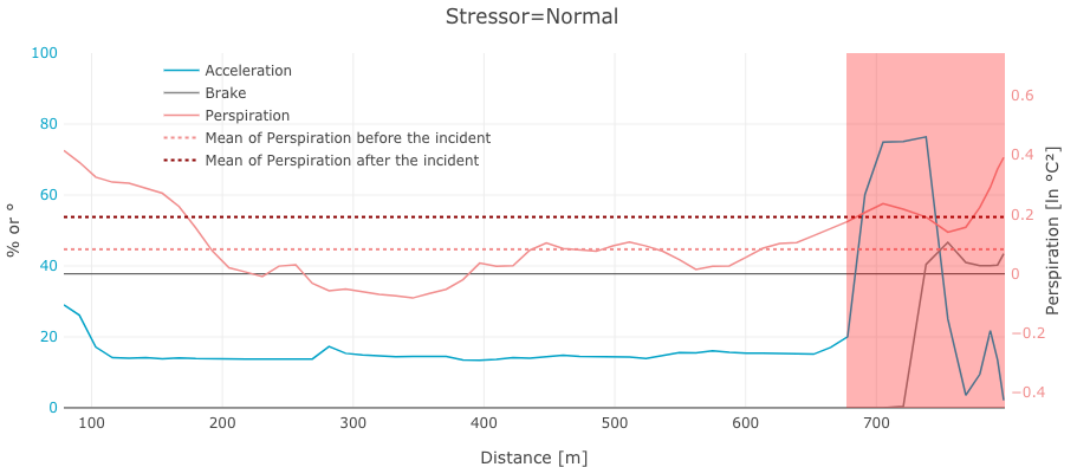

FIGURE B.7: Failure Drive of Subject #07

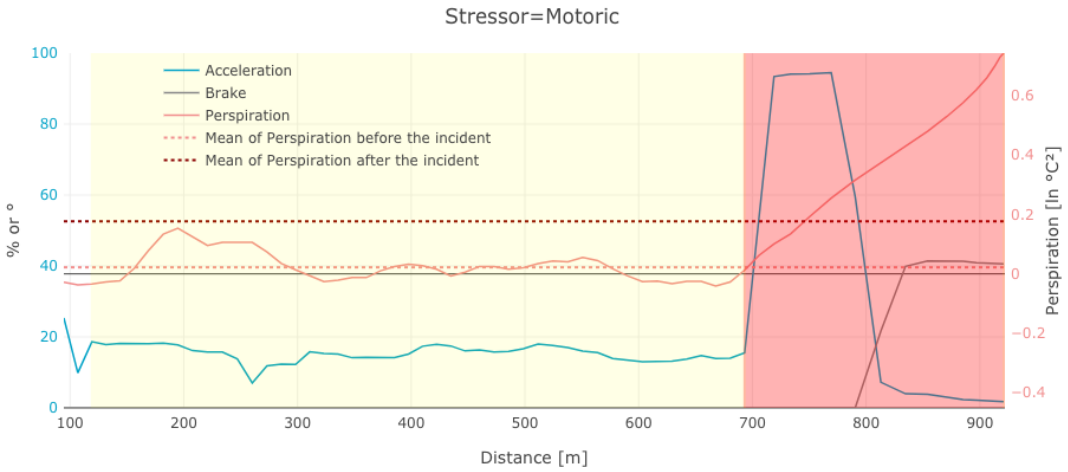

FIGURE B.8: Failure Drive of Subject #09

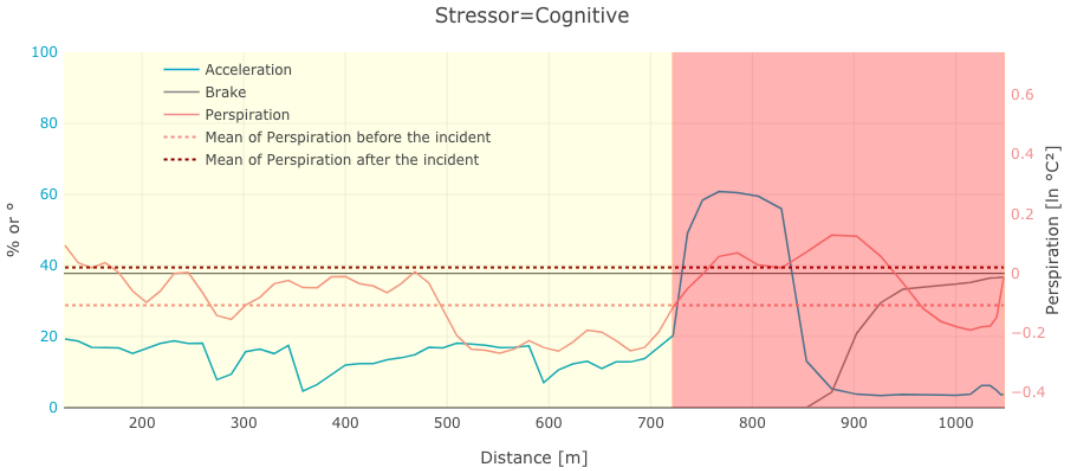

FIGURE B.9: Failure Drive of Subject #12

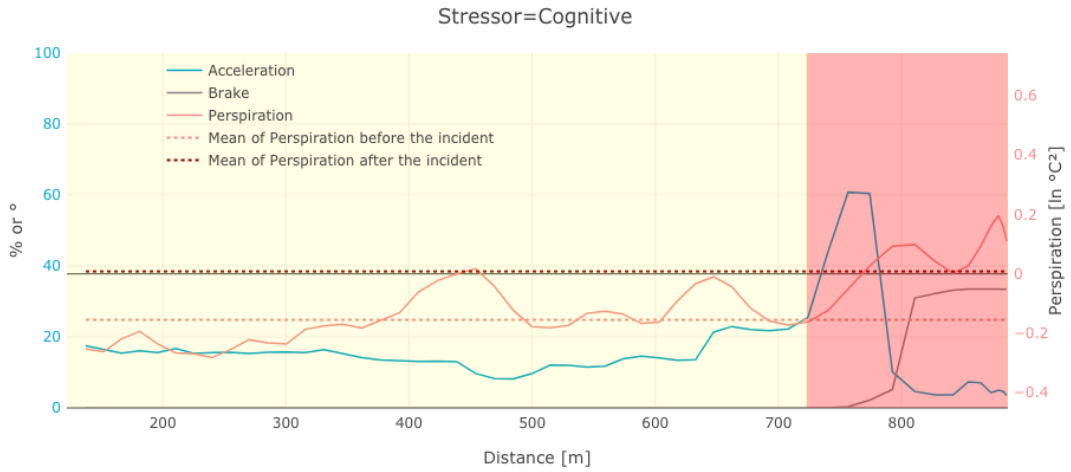

FIGURE B.10: Failure Drive of Subject #13

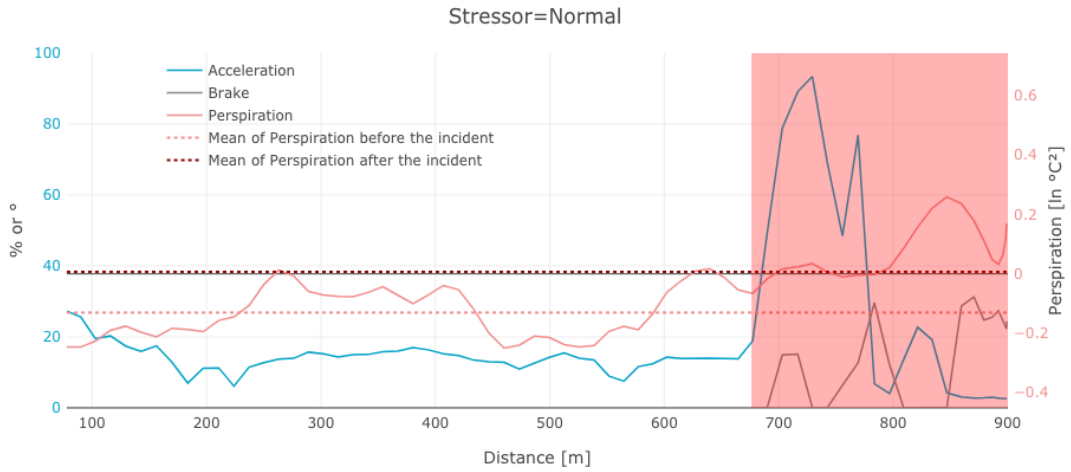

FIGURE B.11: Failure Drive of Subject #15

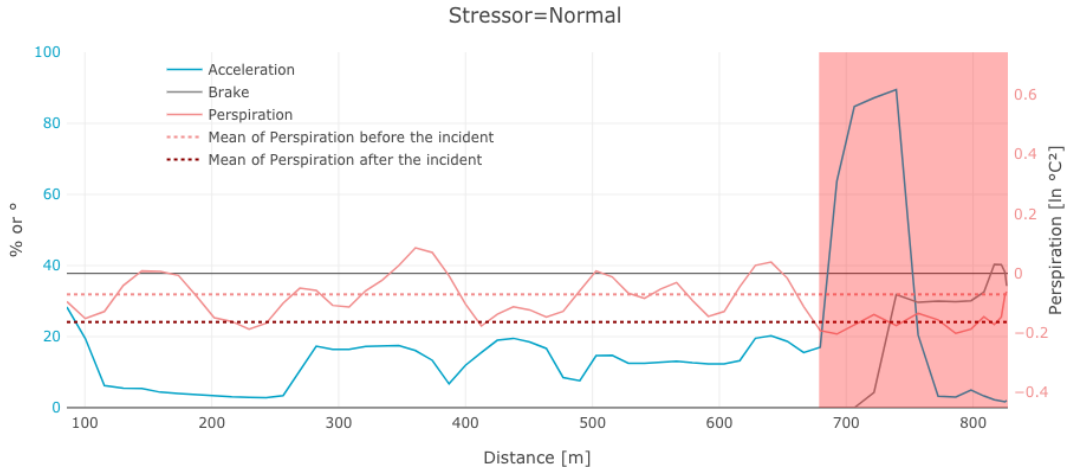

FIGURE B.12: Failure Drive of Subject #16

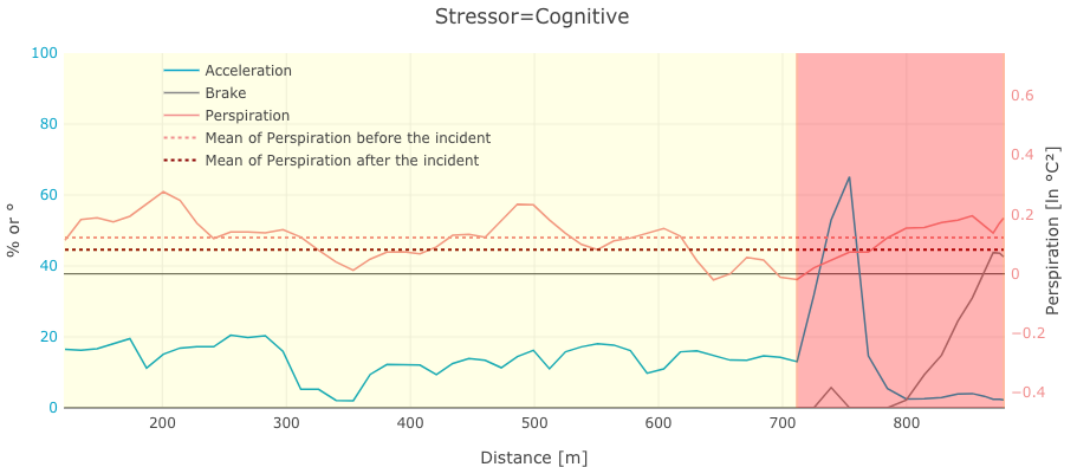

FIGURE B.13: Failure Drive of Subject #17

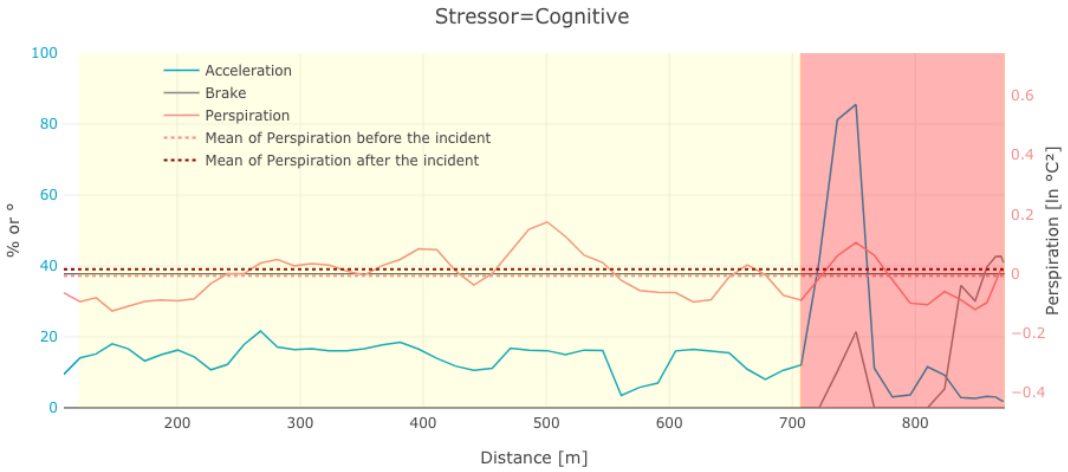

FIGURE B.14: Failure Drive of Subject #18

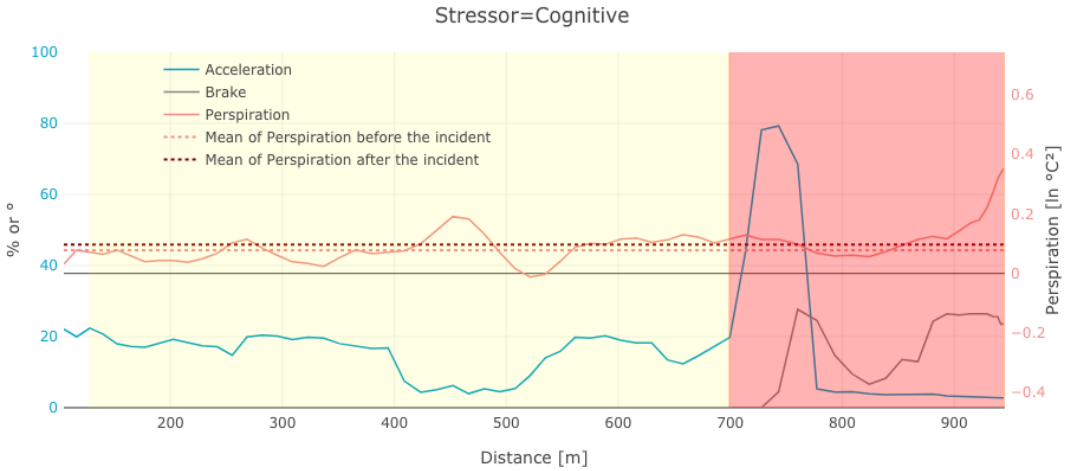

FIGURE B.15: Failure Drive of Subject #22

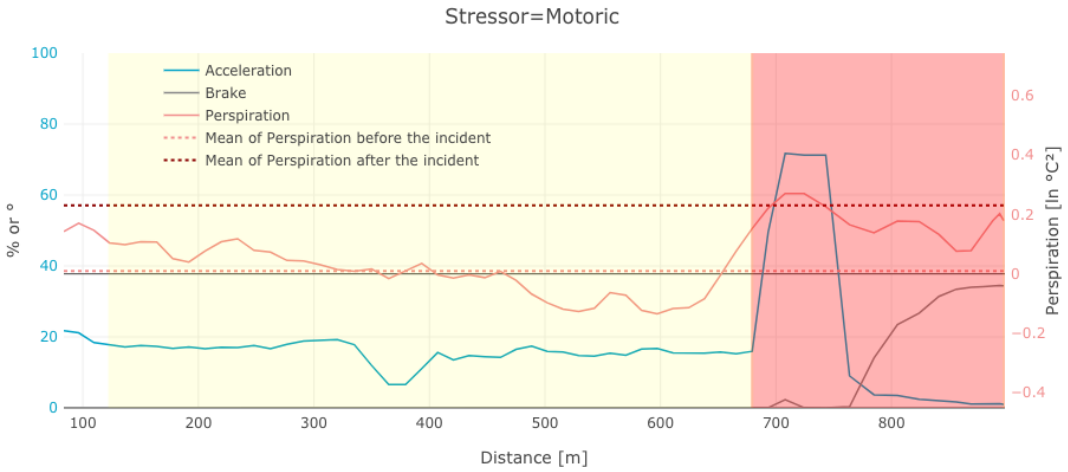

FIGURE B.16: Failure Drive of Subject #24

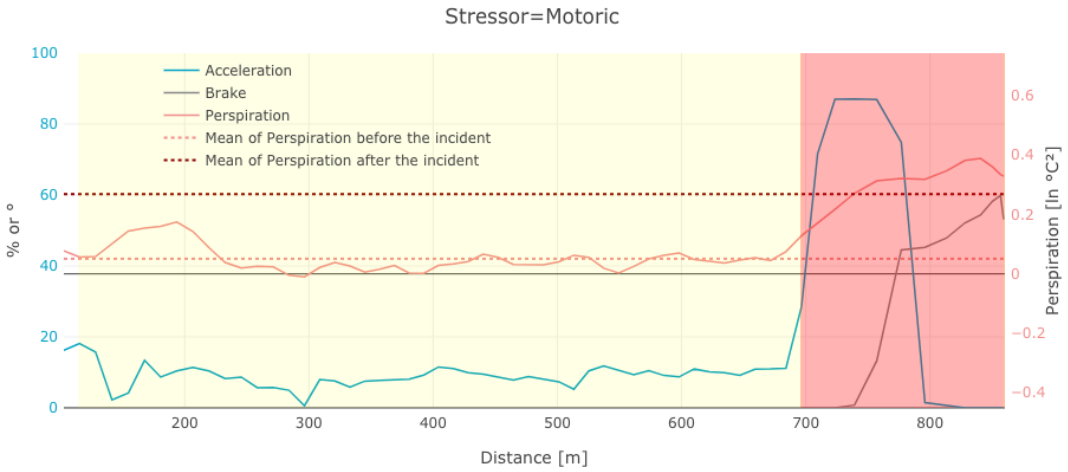

FIGURE B.17: Failure Drive of Subject #29

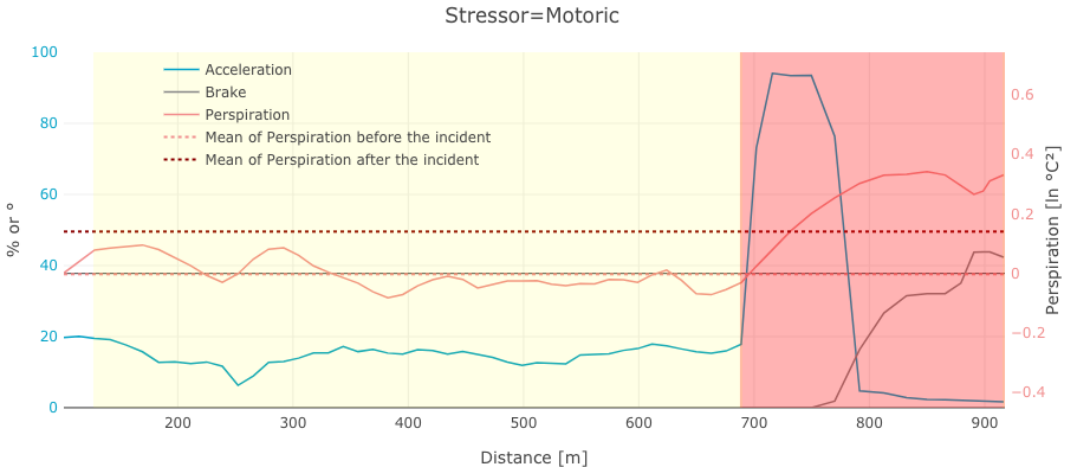

FIGURE B.18: Failure Drive of Subject #30

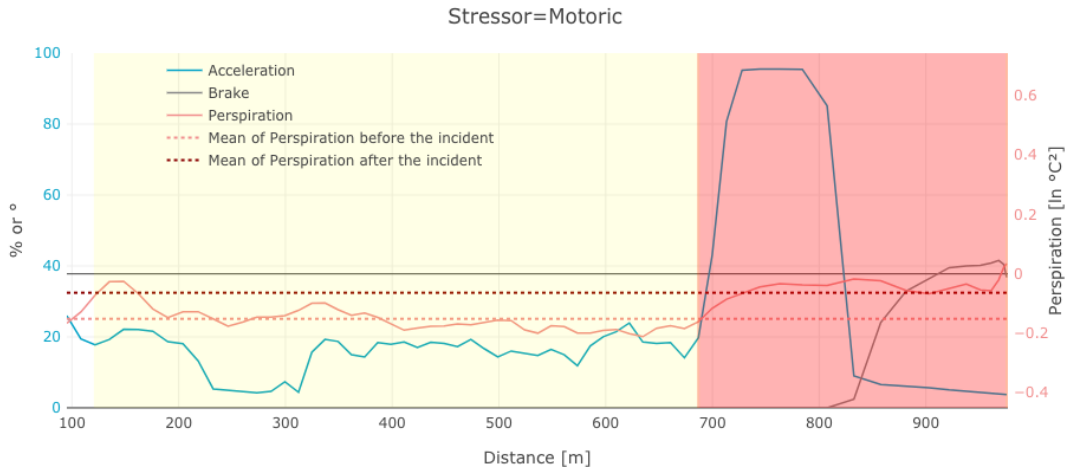

FIGURE B.19: Failure Drive of Subject #31

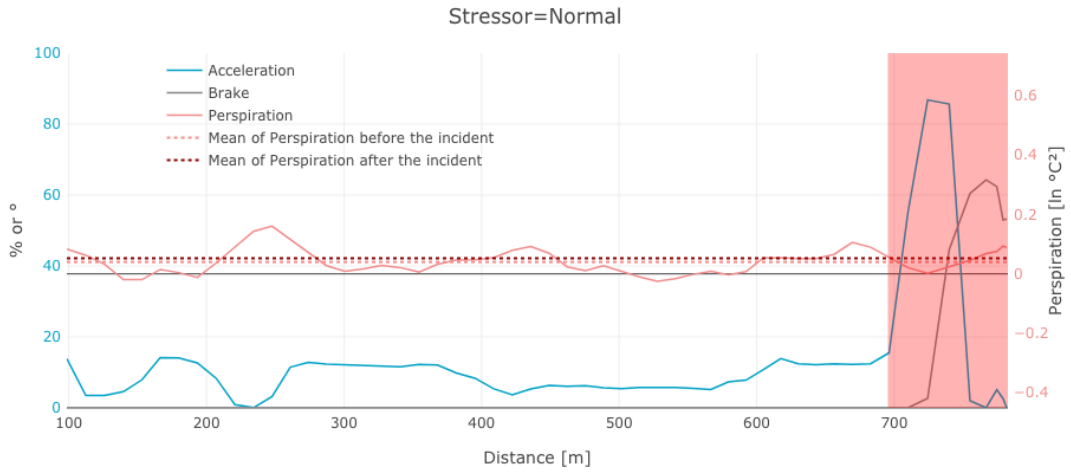

FIGURE B.20: Failure Drive of Subject #32

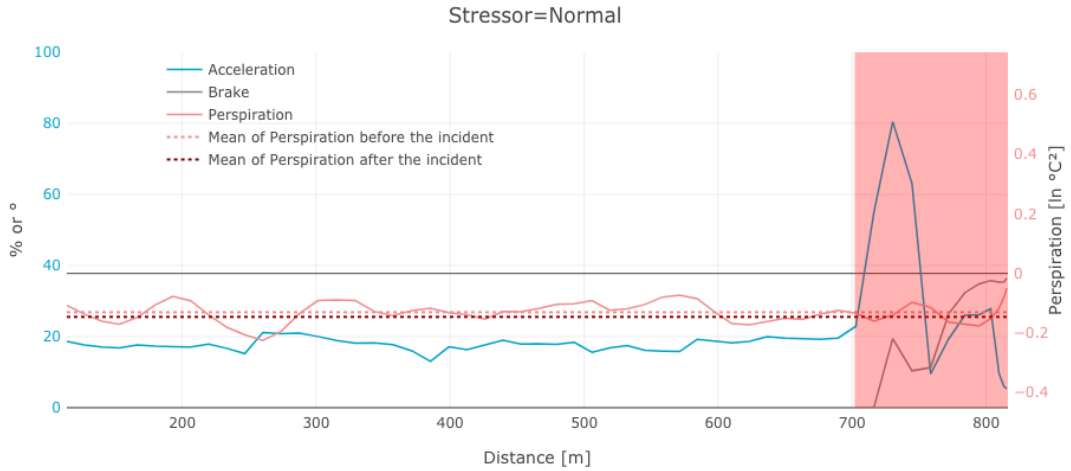

FIGURE B.21: Failure Drive of Subject #41

Bibliography

Baker, Frank B. and Lawrence J. Hubert (1975). "Measuring the Power of Hierarchical Cluster Analysis". In: *Journal of the American Statistical Association* 70.349, pp. 31–38.

Beggiato, Matthias et al. (June 2017). "Lane Change Prediction: From Driver Characteristics, Manoeuvre Types and Glance Behaviour to a Real-Time Prediction Algorithm". In: *UR:BAN Human Factors in Traffic*. Springer Fachmedien Wiesbaden, pp. 205–221.

Chen, Tianqi and Carlos Guestrin (Aug. 2016). "XGBoost". In: *Proceedings of the 22nd ACM SIGKDD International Conference on Knowledge Discovery and Data Mining*. ACM.

Clapp, Joshua D. et al. (Jan. 2011). "The Driving Behavior Survey: Scale Construction and Validation". In: *Journal of Anxiety Disorders* 25.1, pp. 96–105.

Defays, D. (Apr. 1977). "An Efficient Algorithm for a Complete Link Method". In: *The Computer Journal* 20.4, pp. 364–366.

Eboli, Laura, Gabriella Mazzulla, and Giuseppe Pungillo (2017). "How Drivers' Characteristics Can Affect Driving Style". In: *Transportation Research Procedia* 27, pp. 945–952.

Healey, J.A. and R.W. Picard (June 2005). "Detecting Stress During Real-World Driving Tasks Using Physiological Sensors". In: *IEEE Transactions on Intelligent Transportation Systems* 6.2, pp. 156–166.

Huber, Bertold and Reinhard Drews (2009). *How to Use Objective Measurement Data for Vehicle Dynamics Testing*. `https://s3-eu-central-1.amazonaws.com/centaur-wp/theengineer/prod/content/uploads/2013/11/27174300/how_to_use_objective_measurement_data.pdf`. (Accessed on 07/09/2020).

Kaufman, Leonard (2005). *Finding Groups in Data : an Introduction to Cluster Analysis*. Hoboken, N.J: Wiley. ISBN: 978-0471735786.

Kim, Dae-Hwan, Lucie M. Ramjan, and Kwok-Kei Mak (June 2015). "Prediction of Vehicle Crashes by Drivers Characteristics and Past Traffic Violations in Korea Using a Zero-inflated Negative Binomial Model". In: *Traffic Injury Prevention* 17.1, pp. 86–90.

Lucidi, Fabio et al. (Mar. 2019). "Personality Traits and Attitudes Toward Traffic Safety Predict Risky Behavior Across Young, Adult, and Older Drivers". In: *Frontiers in Psychology* 10.

Mohamad, Ismail Bin and Dauda Usman (Sept. 2013). "Standardization and its Effects on K-Means Clustering Algorithm". In: *Research Journal of Applied Sciences, Engineering and Technology* 6.17, pp. 3299–3303.

NHTSA (May 2015). *Safety Advisory: Reducing Crashes Caused by Pedal Error*. `https://www.nhtsa.gov/press-releases/nhtsa-safety-advisory-reducing-crashes-caused-pedal-error`. (Accessed on 07/13/2020).

OpenStreetMap Contributors (2017). *Planet Dump Retrieved from https://planet.osm.org*. `https://www.openstreetmap.org`.

Otsu, Nobuyuki (Jan. 1979). "A Threshold Selection Method from Gray-Level Histograms". In: *IEEE Transactions on Systems, Man, and Cybernetics* 9.1, pp. 62–66.

Panagopoulos, George and Ioannis Pavlidis (Feb. 2020). "Forecasting Markers of Habitual Driving Behaviors Associated With Crash Risk". In: *IEEE Transactions on Intelligent Transportation Systems* 21.2, pp. 841–851.

Park, Sungji, Youngsuk Choi, and Woongchul Choi (Oct. 2016). "Experimental Study for the Reproduction of Sudden Unintended Acceleration Incidents". In: *Forensic Science International* 267, pp. 35–41.

Pavlidis, I. et al. (May 2016). "Dissecting Driver Behaviors Under Cognitive, Emotional, Sensorimotor, and Mixed Stressors". In: *Scientific Reports* 6.1.

Petridou, Eleni and Maria Moustaki (2000). "Human Factors in the Causation of Road Traffic Crashes". In: *European Journal of Epidemiology* 16.9, pp. 819–826.

Ren, Yuan Yuan et al. (2015). "Analysis of Drivers' Eye-Movement Characteristics When Driving around Curves". In: *Discrete Dynamics in Nature and Society* 2015, pp. 1–10.

Rousseeuw, Peter J. (Nov. 1987). "Silhouettes: A Graphical Aid to the Interpretation and Validation of Cluster Analysis". In: *Journal of Computational and Applied Mathematics* 20, pp. 53–65.

Saeed, Aaqib and Stojan Trajanovski (2017). "Personalized Driver Stress Detection with Multi-task Neural Networks using Physiological Signals". In: *CoRR* abs/1711.06116.

Shastri, D. et al. (July 2012). "Perinasal Imaging of Physiological Stress and Its Affective Potential". In: *IEEE Transactions on Affective Computing* 3.3, pp. 366–378.

Shinar, David (1978). *Psychology on the Road : the Human Factor in Traffic Safety*. New York: Wiley. ISBN: 978-0471039976.

Sorensen, H. et al. (1987). "Real-valued Fast Fourier Transform Algorithms". In: *IEEE Transactions on Acoustics, Speech, and Signal Processing* 35.6, pp. 849–863.

Stefano, Marilyn Di, Rwth Stuckey, and Natasha Kinsman (Feb. 2019). "Understanding Characteristics and Experiences of Drivers Using Vehicle Modifications". In: *American Journal of Occupational Therapy* 73.1, 7301205050p1.

Stone, M. (Jan. 1974). "Cross-Validatory Choice and Assessment of Statistical Predictions". In: *Journal of the Royal Statistical Society: Series B (Methodological)* 36.2, pp. 111–133.

Tsiamyrtzis, Panagiotis et al. (May 2016). "Delineating the Operational Envelope of Mobile and Conventional EDA Sensing on Key Body Locations". In: *Proceedings of the 2016 CHI Conference on Human Factors in Computing Systems*. ACM.

Zaman, Shaila et al. (2019). "Stress and Productivity Patterns of Interrupted, Synergistic, and Antagonistic Office Activities". In: *Scientific Data* 6.1, p. 264. ISSN: 2052-4463.

Zhou, Yan et al. (May 2013). "Spatiotemporal Smoothing as a Basis for Facial Tissue Tracking in Thermal Imaging". In: *IEEE Transactions on Biomedical Engineering* 60.5, pp. 1280–1289.